Waitaha Hydro Project - Downstream Flow Modelling

Downstream Flow Modelling

4 June 2025

AusHydro

Document Information

Project	Waitaha Hydro Project
Document Title	Downstream Flow Modelling
Client Contact	[redacted]
Project Director	Rodger Griffiths

Revision History

Revision	Author	Review / Approved	Release Information
DRAFT	Dougal Clunie	Jeremy Kent-Johnston	20 Feb 2025
DRAFT 2	Dougal Clunie	Jeremy Kent-Johnston	25 Feb 2025
1	Dougal Clunie	Jeremy Kent-Johnston	04 April 2025
2	Dougal Clunie	Jeremy Kent-Johnston	28 April 2025
3	Dougal Clunie	Jeremy Kent-Johnston	7 May 2025
4	Dougal Clunie	Jeremy Kent-Johnston	4 June 2025

Disclaimer:

This document is provided solely for information related to downstream flow modelling for the Waitaha Hydro Project. The document is limited to the matters set out within and is subject to the stated scope, assumptions, qualifications, exclusions and limitations. Any assumptions in this document are based on information available at the time of preparation and may not reflect subsequent developments.

The development of this document may have included input, work or assistance from third parties and no reliance is placed on such input, work or assistance. No representation is made that the scope, assumptions, qualifications, exclusions or limitations are suitable or sufficient for purposes beyond this Project. This document may not cover all matters the recipient considers material.

Unless expressly agreed in writing, this document and any excerpts must not be distributed or copied to any third party. This document supersedes all previous drafts or interim versions, whether written or presented orally, issued during the Project lifecycle.

Executive Summary

2D computational hydraulic modelling was undertaken to investigate the response of Waitaha River flows following rapid changes of discharge from the power station, including load rejection (i.e. sudden loss of power generation) and station startup and shutdown.

This report presents indicative transient changes in flow rate and depth at different locations along the river, to inform environmental effects and public safety risk assessments being undertaken by others. The modelling and results presented are based on uncalibrated computational modelling and so should be considered as indicative as opposed to precise, and appropriate conservatism should be used when applying model outcomes.

Three river flow scenarios were modelled, including the worst-case for flow change where the power station is at maximum discharge of 23 m^3/s whilst the headworks are passing minimum residual discharge of 3.5 m^3/s. Higher and lower river conditions were also modelled, spanning some 40% of the expected river flow range.

For each of the three river conditions, three power station scenarios were modelled in response to load rejection, including rapid shutdown of full flow, and rapid transition to a bypass valve discharge of 10 or 15 m^3/s. Scenarios for controlled full station shutdown (ramp-down times of 30, 45 and 60 minutes) and full station load acceptance (ramp-up times of 10 and 30 minutes) were also modelled.

The hydraulic effect of these scenarios was reviewed at two main locations:

- Downstream of the power station, including braided reaches. The modelled reach extended some 7.5 km downstream of the power station and was assessed to understand flow change and potential for adverse ecological impacts such as fish stranding.
- Within Morgan Gorge, particularly at the hot spring location approximately 800 m downstream of the proposed diversion weir. The purpose was to assess water level change, travel times, and associated flood hazard, to aid in understanding the potential public safety impact.

The key findings at both locations were as follows:

Downstream reach:

- Following load rejection there is a temporary reduction in river flow rate and water level downstream of the station, with a modelled lag time (over which rejected flow spills over the headworks and flows down the gorge) ranging from 30 to 40 minutes before recovery of the steady-state flow just downstream of the power station.
- As this temporary flow deficit travels downstream, significant attenuation occurs, limiting the effects of the initial load rejection. For example, at worst case river conditions there is an 80% flow reduction immediately downstream of the station (Figure-ES1) which attenuates to a 50% flow reduction 7.5 km downstream.
- Modelling indicates that water level and flow rate in the braided reach drop temporarily following load rejection, but flow is maintained in all braids.

- Depth changes throughout the reach are significantly lower in the scenarios with a bypass valve due to the smaller sudden drop in power station flow discharge.
- For slower controlled station shutdown there is a similar temporary flow deficit downstream of the station, though the drop in flowrate, depth, and rates of change of flow is not as great as for a load rejection with no bypass. The magnitude of flow drop reduces with longer shutdown times.
- For station startup there is a temporary increase in flow downstream of the station, the magnitude of which reduces with longer startup times (e.g. Figure 5-11).

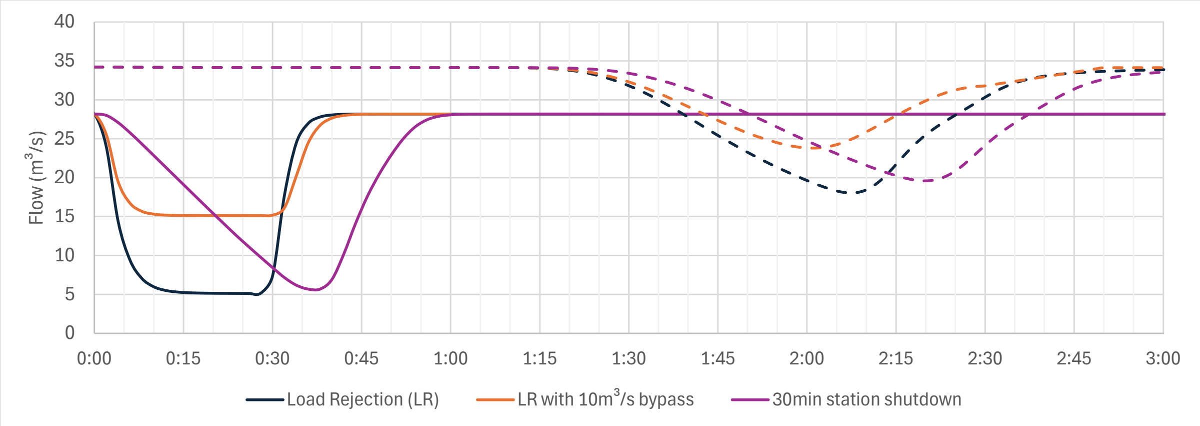

Figure ES1: Flow changes following load rejection and station shutdown (a) 100 m downstream of the station (solid lines) and (b) 7.5 km downstream (dashed lines) noting an increased steady-state flowrate due to tributary inflows. 26.5 m^3/s river flow condition.

Flood hazard in Morgan Gorge and at Hot Spring:

- A hot spring discharges onto a rock ledge above the river within Morgan Gorge, an area known to be visited by members of the public.
- Modelling indicates that the hot spring rock ledge becomes naturally inundated at river flows of around 50 m^3/s and above, which occur about 10% to 15% of the time.
- Following full station load rejection, the maximum river level rise (at lowest full-station river conditions, i.e. $Q_{WAITAHA}$ = 26.5 m^3/s) at the hot spring is 0.75 m, which is reduced to less than 0.50 m if a 10 m^3/s bypass valve is operated at the station.
- At the highest river conditions during which people could reasonably be expected to be at the hot spring (i.e. water just below the ledge, full station discharge, $Q_{WAITAHA}$ = 42 m^3/s), load rejection without a bypass would lead to inundation of most of the rock ledge. Inundation depths would be up to 0.5 m and velocities up to 2 m/s, and the depth-velocity product (DV) generally 0.2-0.4 m^2/s constituting a low hazard for adults following the thresholds described in Smith et al (2014). At this river condition with a 10 m^3/s bypass valve operating, the water level rise is reduced, the ledge is only partially inundated and DV on the inundated parts of the ledge is limited to 0.2 m^2/s.
- The flow increase at the hot spring location occurs around 10 minutes after flow rejection at the power station and rises over 4 minutes.
- Following load rejection from a minimum residual flow, there are small, scattered (originally dry) areas within the gorge which become inundated, some with 'moderate hazard' (DV > 0.6, refer Section 6.7) in the no-bypass scenario, but minimal areas with DV above 0.6 for scenarios with a bypass valve operating.

A bypass valve maintains some flow continuity from the power station following load rejection. This reduces the flow deficit downstream, and reduces the flow increase within the bypassed gorge reach. Reducing these rapid flow changes will reduce effects on aquatic fauna and reduce potential safety risks for people on or near the river.

The flood hazard level within the gorge in a load rejection scenario is low, even with no station bypass, given the:

- elevated setting of the hot spring,
- relatively low inundation depths and velocities in worst-case conditions, and
- relatively small areas of hazardous inundation depth/velocity elsewhere in the gorge.

The associated public safety risk is probably very low considering the low expected joint probability of the presence of people coinciding with a load rejection event.

Given the uncalibrated basis of the model, and known limitations in the modelled terrain, model outcomes should be applied with conservatism. The low (but slightly uncertain) flood hazard level can be further reduced by the inclusion of a bypass valve at the power station. Therefore, it is recommended that allowance for a 10 m^3/s bypass valve is included in the power station design.

It is recommended that the environmental effects and personnel safety risk of rapid power station flow changes are assessed based on the information provided in this report.

If desired, further field data collection could be undertaken to allow more precise modelling and confirm the need for a bypass valve.

AusHydro

Contents

1 Introduction

1.1 Background

The Waitaha Hydro Project (the Project) is a proposed run-of-river hydropower project on the Waitaha River on South Island's West Coast. The Project proposes to divert up to 23 m^3/s of water from the downstream end of Kiwi Flat (immediately upstream of Morgan Gorge) through a tunnelled waterway to a power station on the bank of the Waitaha River some 2.6 km downstream.

Australian Hydropower Pty Ltd (AusHydro) was commissioned by Westpower Ltd in January 2024 to provide engineering design services for the Project.

1.2 Purpose of this Report

This report outlines 2D computational hydraulic modelling undertaken to investigate the response of Waitaha River (flows and water levels) following rapid change of discharge from the power station, including:

- Sudden flow decrease following load rejection (i.e. loss of power generation) at the power station, and
- Controlled ramp-up/down of flow, e.g. station startup or shutdown, shutdown of flow bypass valve.

The report presents indicative transient changes in flow rate and depth at different locations along the river, to inform environmental effects and public safety assessments being undertaken by others. In addition, flow and depth changes within the bypassed Morgan Gorge reach of the river are presented, to assess the flood hazard associated with the sudden increase in flow within the gorge, and at the hot spring location in particular, following load rejection.

The modelling results presented are based on uncalibrated computational modelling and so should be considered as indicative rather than precise. Limitations of the modelling are further discussed in Section 4.

1.3 Description of the Waitaha River

The Waitaha River is located 38 km south of Hokitika, with a total catchment area of 223 km^2 rising to around 2,200 m elevation.

The Project intake is at the head of Morgan Gorge, with a catchment area of 116 km^2. Average flows are in the order of 35 m^3/s at the intake, with a median flow of around 18 m^3/s. The catchment experiences intense rainfall, with a mean annual flood estimated at 812 m^3/s.

Downstream of the proposed intake site at Kiwi Flat, the steep and narrow Morgan Gorge extends for around 1 kilometre though schist bedrock. Downstream the river slope flattens with the riverbed comprising alluvial boulders and gravels supplied by the Waitaha and steep tributary streams. Downstream of MacGregor Creek (from approximately 5 km downstream of Kiwi Flat) the active riverbed widens with the flow splitting into multiple braided channels.

A long-section of the river water surface from LiDAR topography, covering the reach assessed in the present modelling, is shown in Figure 1-1. Throughout this report, river locations are identified by 'chainage', the distance downstream from the headworks weir along the river centreline.

For reference, the SH6 highway bridge is at chainage 19,000 m, 8.6 km downstream from the modelled reach, with the coast a further 3.8 km downstream.

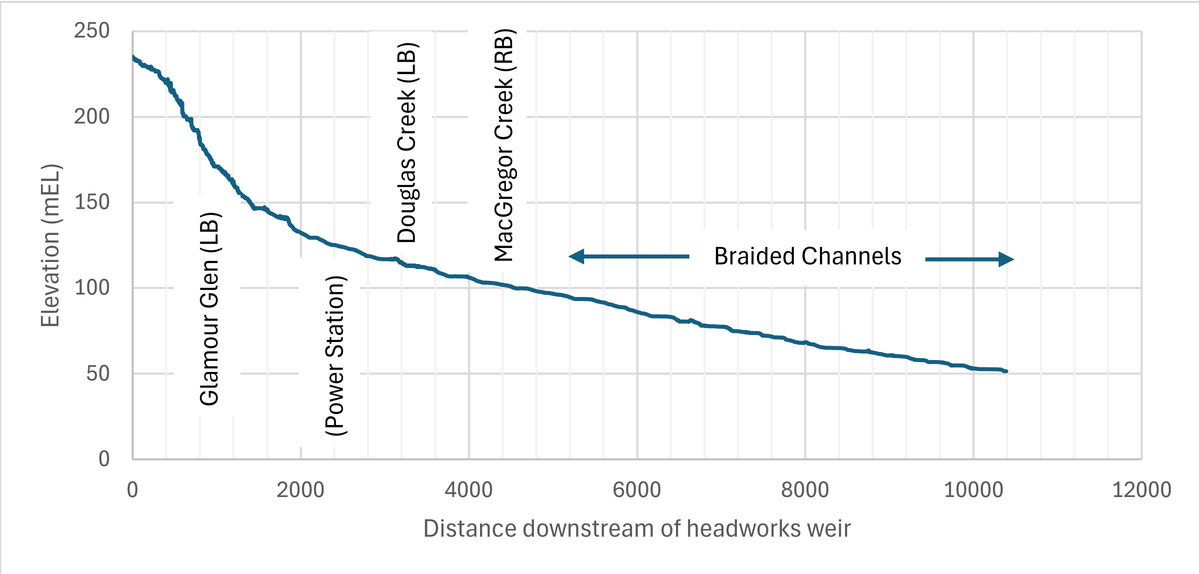

Figure 1-1: Long-section of Waitaha River, with significant tributaries identified

With a rapid decrease of flow from the power station, flows in the river downstream will temporarily reduce. River inflows from Kiwi Flat will raise the ponded water level and overtop the diversion weir, quickly increasing flow within the gorge, and after a short time 'catch-up' and restore the original flow rate in the river downstream of the station.

For a rapid increase in power station flow the opposite occurs, with flows into the gorge decreasing and flow in the river downstream of the station temporarily increasing before the flow deficit 'catches up' and restores the original flow rate in the river downstream.

2 Model Setup

2.1 Overview of Model

Two-dimensional (depth-averaged) computational hydraulic modelling of the Waitaha River was undertaken using HEC-RAS 6.5 software.

The modelled domain extends from Kiwi Flat for approximately 10 km downstream, as shown in Figure 2-1.

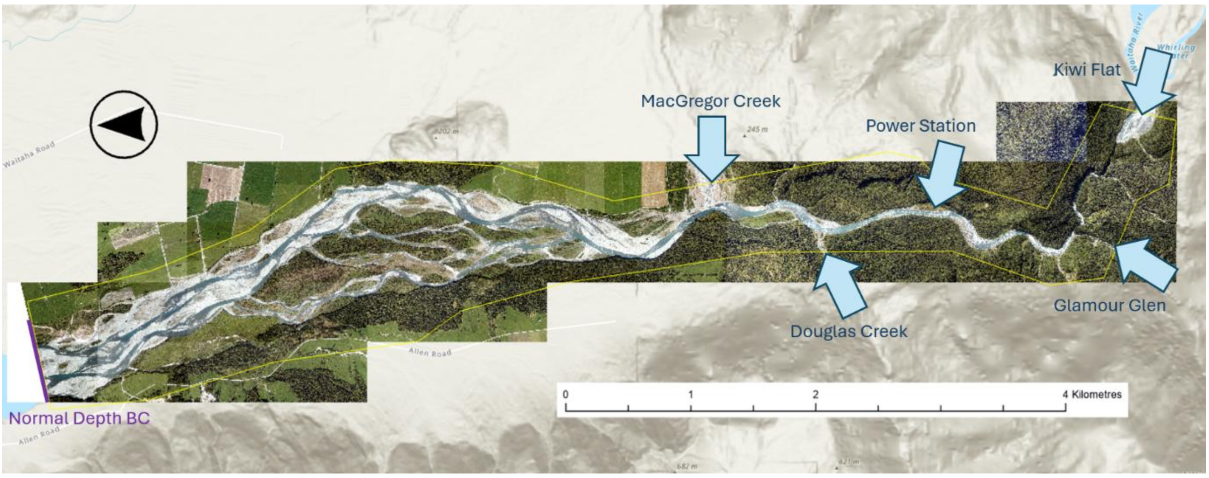

Figure 2-1: Modelled domain and boundary conditions

2.2 Model Boundary Conditions

The model includes five inflow boundaries, and a normal depth (slope = 0.01) boundary at the downstream end. The tributary flow rates were calculated from a proration of catchment areas (with contributing areas shown in Figure 2-2).

The model was run for three Waitaha River flow rates ($Q_{WAITAHA}$) as described in Section 3.

Inflow boundaries were included at the following locations:

- Power Station (Q_{PS})
- Kiwi Flat ($Q_{WAITAHA}$ - Q_{PS})
- Glamour Glen ($Q_{INTERMEDIATE} = 0.061 \times Q_{WAITAHA}$)
- Douglas Creek ($Q_{DOUGLAS} = 0.084 \times Q_{WAITAHA}$)
- MacGregor Creek ($Q_{MACGREGOR} = 0.142 \times Q_{WAITAHA}$)

Flow within the proposed waterway tunnel was not explicitly modelled, instead flow changes at the power station were matched by corresponding flow changes at Kiwi Flat one minute later. This time nominally represents the time for flow to cease within the tunnel (a few seconds), and surges to balance such that the headpond level begins to increase.

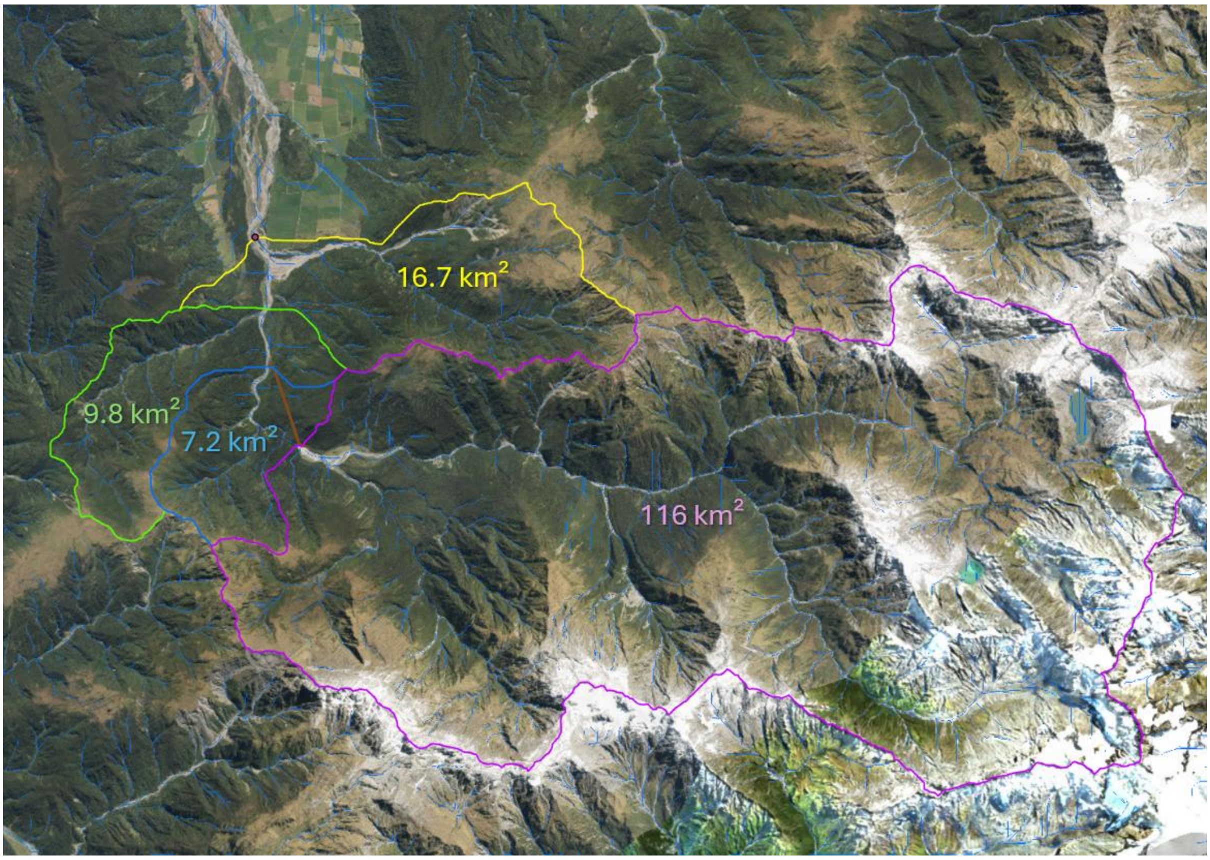

Figure 2-2: Catchments of Waitaha River at headworks 116 km^2, intermediate catchment to power station 7.2 km^2, Douglas Creek (including Alpha Creek on right-bank 9.8 km^2, MacGregor Creek (including Granite Creek) 16.7 km^2

2.3 Model Terrain

The model terrain was based on LiDAR topographic data captured by Landpro on 3 Nov 2024.

LiDAR-based topography captures the water level surface elevation, as opposed to the elevation below the water-surface (bathymetry). Therefore, the channel bathymetry is not well represented and needed to be accounted for. On the day of capture, the Hokitika River at Gorge measured a flow of 114 to 87 m^3/s, receding following rainfall on 1 November 2024. From the correlation reported by Doyle[1], the Waitaha River flow at the time of the LiDAR capture is assumed to be 22-29 m^3/s, around a 30% exceedance level (i.e. highish).

Within Morgan Gorge the model terrain was modified by subtracting estimated flow depths from the observed water surface extents. The modified terrain provides a better representation of gorge hydraulics (i.e. storage, flow conditions, head loss), and improves estimates for travel times. Water depths were estimated at sections at 5 m intervals throughout the gorge, based on initial model runs and verified by comparing remodelled flow against aerial imagery and measured water surface elevations.

The terrain was further modified by inclusion of a weir structure at proposed headworks location, and the tailrace channel at the proposed power station location.

[1] Based on correlation in Doyle Hydrology Report Appendix D

2.4 Computational Grid

The model uses an unstructured computational mesh with a 5 m grid in the area of interest from Kiwi Flat to some 3.3 km downstream of the power station. A coarser 15 m mesh is used to modelling the river for a further 3.7 km (altogether some 35,000 computational points). The mesh size is a balance between model accuracy and computational runtime.

2.5 Modelled Roughness

HEC-RAS 2D uses a Manning's *n* roughness coefficient to represent the resistance to flow in the river channel. This is an important parameter for calculating flow depth and the 'travel time' of flow changes. Model sensitivity runs show that with higher *n,* the depth for a given flow is greater, and travel times are increased. In other words, the downstream flow deficit lasts longer following a power station load rejection event.

Empirical formulae are available to provide a rough-order estimate of an appropriate Manning's n. Jarrett (1984) collected extensive field data on steep streams in the Rocky Mountains, and from a regression analysis developed the equation $n = 0.39S^{0.38}R^{-0.16}$. For the Morgan Gorge reach (slope S=0.05) at small depths (hydraulic radius R≈1 m), this suggests n in the order of 0.12, and for the lower reach (S=0.009) n in the order of 0.06.

A calibrated one-dimensional hydraulic model of the Waitaha River reach between Alpha Creek and Donald Creek was developed for IFIM habitat assessment studies using measured cross-sections and flow gauging. From this, the estimated Manning's n was approximately 0.14-0.17. [2]

The Morgan Gorge reach of the river is very steep, and the bed is dominated by large boulders and rock ledges. Further downstream the river slope flattens but the riverbed remains boulder-dominated until receiving significant quantities of gravels from the Douglas Creek and MacGregor Creek tributaries. It is expected that the appropriate Manning's *n* roughness should decrease as both the river slope and size of bed material decreases.

For the model runs, a spatially-varied Manning's n is used, 0.06 at Kiwi Flat, 0.15 within the gorge and downstream to Douglas Creek, 0.10 between Douglas Creek and MacGregor Creek, and 0.06 from MacGregor Creek downstream (Figure 2-3).

Figure 2-3: Manning's n roughness coefficients adopted

[2] M Hicks (personal communications, February 2025)

These roughness values appear consistent with examples presented in Hicks and Mason (1998), reproduced in Appendix A.

The roughness values have not been adjusted to match recorded water levels, as no suitable records of flow and depth along the modelled reach are available, i.e. the model is uncalibrated.

Results from model sensitivity runs, with Mannings *n* roughness 25% greater and 25% less are included in Appendix B. These show that:

- higher roughness produces greater changes in flow depth for a given change in flow rate.
- higher roughness results in longer 'travel times' for flow changes, and
- higher roughness results in a quicker smoothing of flow changes,
- and *vice versa* for low roughness.

The assumed roughness values used for the modelling are 'best estimates' based on-site inspections and previous experience and not deliberately high (to be conservative for greater depth changes) nor low (to be conservative for more rapid flow changes). Given the inherent uncertainty in uncalibrated modelling (see Section 4 for further discussion), conservatism should be applied to the interpretation and use of model outcomes.

3 Modelled Flow Scenarios

3.1 Power Station Flow Cases

Rapid flow changes from the power station will result in flow changes within the bypassed river reach, and temporary flow changes in the river downstream. Three main situations will result in rapid flow changes, and are considered in the modelling, namely:

1. Sudden flow decrease (load rejection):
   - A consequence of loss of power generation (e.g. loss of transmission line connection) at the power station.
   - The wicket gates or main inlet valve closes to protect the station, typically in less than one minute (closure rate related to water hammer effects and allowable periods for overspeed operation), with resultant sudden decrease in station discharge.
   - 'Rejected' water overflows the weir at the head works, and must travel through the gorge, before catching up and re-balancing flow conditions.
2. Controlled flow decrease (operation):
   - Controlled reduction in station discharge, such as station shutdown or shutdown of a flow bypass valve.
3. Controlled flow increase (operation):
   - Controlled increase in station discharge, such as station startup.
   - For the present modelling a steady linear ramping up of flow has been considered, but in reality the flow rate change will be stepped, as a unit is brought up to synchronous speed-no-load (around 10% unit flow) and then quickly ramped up into its normal operating range (around 40% unit flow) before increasing with a controlled ramp rate.
   - The modelled scenarios of load increase from zero to full station output represent an unusual operational case. During normal operation flow changes will generally be much smaller.
   - Rapid increase of flow discharge from the station, and corresponding decrease in flow rate over the weir at the headworks, which takes time to propagate through the gorge, before catching up and re-balancing downstream flow conditions.

Table 3-1: Modelled flow cases

Scenario	Category	Description
Case 1: Full flow rejection	Load Rejection	• Power station discharge reduced to zero linearly in one minute, with corresponding increase in modelled river inflow to Kiwi Flat.
Case 2: 10 m^3/s bypass valve		• Power station reduced to 10 m^3/s linearly in one minute, with corresponding increase in inflow to Kiwi Flat. • 10 m^3/s represents the size of bypass valve that could be included in the scheme design branching off one of the unit penstocks. • This flow case also represents the alternative case where the turbines are allowed to rotate into overspeed which throttles discharge.
Case 3: 15 m^3/s bypass valve		• Power station discharge reduced to 15 m^3/s linearly in one minute, with corresponding increase in inflow to Kiwi Flat. • This case is included to demonstrate the sensitivity of river changes to a larger bypass. In practice this would likely necessitate two bypass valves i.e. one branching off each unit penstock.
Case 4: 30 minute shutdown	Normal shutdown	• Power station discharge reduced to zero linearly over 30 minutes, with corresponding increase in inflow to Kiwi Flat. • For the full station design flow of 23 m^3/s this corresponds to a ramping rate of 0.77 m^3/s per minute.
Case 5: 45 minute shutdown		• Power station discharge reduced to zero linearly over 45 minutes, with corresponding increase in inflow to Kiwi Flat. For the full station design flow this corresponds to a ramping rate of 0.51 m^3/s per minute.
Case 6: 60 minute shutdown		• Power station discharge reduced to zero linearly over 60 minutes, with corresponding increase in inflow to Kiwi Flat. For the full station design flow this corresponds to a ramping rate of 0.38 m^3/s per minute.
Case 7: 10 minute startup -	Startup / Load acceptance	• Power station discharge increased linearly from zero over 10 minutes, with corresponding decrease in inflow to Kiwi Flat. • For the full station design flow of 23 m^3/s this corresponds to a ramping rate of 2.3 m^3/s per minute.
Case 8: 30 minute startup		• Power station discharge increased linearly from zero linearly over 30 minutes, with corresponding decrease in inflow to Kiwi Flat. • For the full station design flow this corresponds to a ramping rate of 0.77 m^3/s per minute.

In Cases 2 and 3, where a bypass valve is operated to reduce the magnitude of sudden flow change from the power station, the bypass valve must be subsequently closed off. This results in a second flow change, which will be similar in nature to normal shutdown Cases 4-6, though for the smaller bypass flowrate. This second flow change from the bypass closure has not been explicitly modelled for all flow scenarios, but a single scenario is shown in Figure 5-1 to demonstrate the effect.

3.2 Waitaha River Conditions

The modelling has investigated the river conditions in which the largest magnitudes of flow and water level changes will occur.

Following load rejection, the worst-case flow deficit (and water level changes) in the river occurs when:

- Power station is at maximum discharge of 23 m^3/s
- Headworks are passing minimum residual discharge of 3.5 m^3/s
- Waitaha River inflow at Kiwi Flat is 26.5 m^3/s

Three river flow conditions were modelled, including this worst case, and higher and lower river conditions spanning some 40% of the expected river flow range.

Table 3-2: River flow conditions modelled, showing for each the maximum station flow Q_{PS} and minimum residual flow past the headworks weir $Q_{RESIDUAL}$

Scenario	$Q_{WAITAHA}$	Q_{PS}	$Q_{RESIDUAL}$	Notes
1	26.5 m^3/s	23 m^3/s	3.5 m^3/s	approx. 27% exceedance
2	16.5 m^3/s	13 m^3/s	3.5 m^3/s	Nominal lower flow ~56% exceedance
3	36.5 m^3/s	23 m^3/s	13.5 m^3/s	Nominal higher flow ~17% exceedance

3.3 Modelled Scenarios

For each of the three river conditions described in Table 3-2, the eight power station flow cases have been modelled.

Shutdown and startup flow cases have modelled the ramp-down or up of the full station flow (i.e. Q_{PS} from Table 3-2), noting that these represent unusual operation, and during normal operation flow changes will typically be small following run-of-river.

The modelling of the above scenarios focussed on assessment of flow changes at two main locations:

- Downstream of the power station (outcomes presented in Section 5).
- At the hot spring located toward the downstream end of Morgan Gorge. (Section 6).

4 Model Limitations

There are certain limitations with all computational hydraulic models. Some limitations which are relevant to this study are listed below:

- The model terrain is based on LiDAR topography, with the modelled riverbed being at the level of the water surface on the day of data capture. Within the gorge reach, the terrain has been adjusted based on inferred flow depths from depth and velocity calculated in preliminary model runs to mitigate the effect of the 'baked-in' water surface. In downstream areas modelled water levels will be higher than reality.
- The model terrain is essentially a 'snap-shot' in time, and cannot account for any changes in flow path that might occur as a consequence of future flood flows and associated erosion and deposition of gravels.
- The 2D model will not directly represent features within the river channel smaller than the scale of the mesh element areas.
- Assumptions regarding channel surface roughness (i.e. Manning's n values) were made based on-site inspections and previous experience. There are no suitable records of flow and river stage across the model extent to validate them. The surface roughness itself is a simplification of flow processes driven by local (sub-mesh size) riverbed features, which have been assumed to be similar over the regions of different roughness modelled.
- The modelling does not account for subsurface flows within the gravel riverbed.
- Tributary inflows are based on a simple ratio at catchment area and lumped into a limited number of discrete inflow points. During a site visit in February 2025 it was apparent that some larger tributaries appeared 'dry' (some flowing beneath the coarse gravel bed, with flowing surface water visible further upstream) while surface inflows were apparent at other small tributaries and other locations with negligible topographic catchment.

Whilst these limitations mean that model results should be considered 'indicative' only, the modelled flow dynamics (e.g. water level changes, travel times etc.) provide worthwhile information for assessing effects.

The model has been applied conservatively with worst-river case conditions for flow change investigated. Model roughness parameters, which have a significant effect on flow depth for given flow rates, are best estimates based on site inspections and previous experience, i.e. the model is uncalibrated.

Given the uncalibrated model roughness and other model limitations described above, conservatism should be applied to the interpretation and use of model outcomes.

If more precise estimates of flow changes are required (e.g. if applying conservatism may be uneconomic or otherwise undesirable), then field data should be collected to verify the modelled relationships between river flowrate and water depth.

5 Downstream of Power Station

The Waitaha Hydro Project is a run-of-river scheme, meaning that river inflows are not stored for the purposes of scheme operation. Operational flow changes will typically be gradual, in response to changes in river inflows.

In the unusual (i.e. expected, but not occurring frequently) operational cases modelled, flows from the power station are rapidly changed, with the corresponding rapid change in river flow propagating downstream. The flow change is temporary, as changes in flow taken by the station are matched by an opposite change in flow over the headworks diversion weir, with this flow travelling via the Morgan Gorge reach and 'catching up' to restore the original flow rate in the river downstream of the station.

The modelled outcomes of rapid reduction in power station flow, following station load rejection are shown in Section 5.1, and for controlled station shutdown in Section 5.2. The modelled outcomes of rapid increase in power station flow following station startup are shown in Section 5.3.

5.1 Station Load Rejection

The modelled flow change at a cross-section a short distance downstream of the power station following load rejection is shown in Figure 5-1. For the three station flow cases modelled, this chart shows the river flow rate reducing after load rejection, then recovering after the rejected flow arrives via the gorge. A key aspect is the lag between load rejection and recovery of the steady-state flow downstream of the power station. The modelled lag period ranges from 30 to 40 minutes.

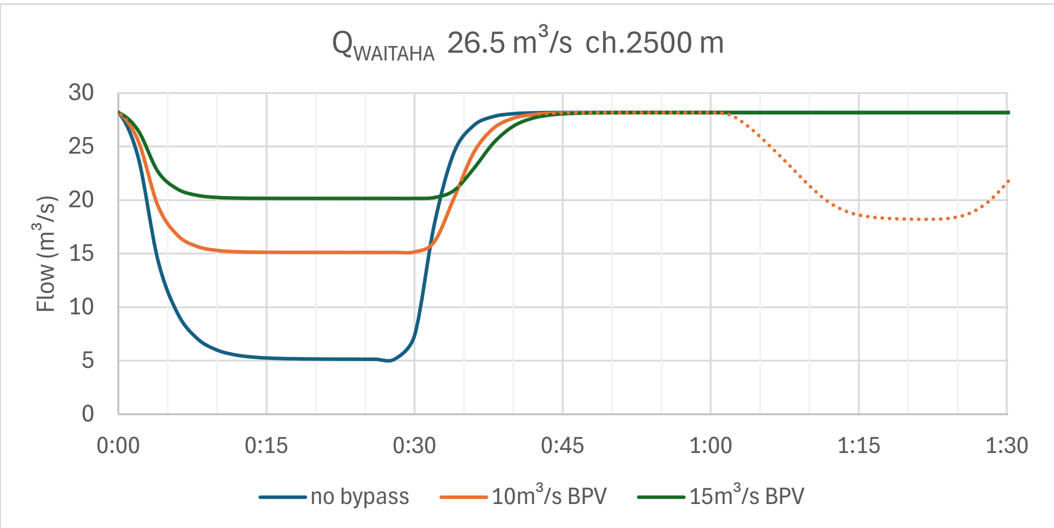

Figure 5-1: Modelled flow in Waitaha River at model chainage 2500 m (100 m downstream of power station) for three power station flow rejection scenarios, $Q_{WAITAHA} = 26.5\ m^3/s$

If a bypass valve is operated to mitigate the reduction in flow from the power station following load rejection, the valve will subsequently need to be closed, with a resultant second flow deficit propagating downstream. The dashed line in Figure 5-1 shows the subsequent shutdown of a 10 m^3/s bypass valve in 10 minutes.

The effects of bypass shutdown are of a secondary order compared to the initial load rejection load, in that the magnitude of change is not as great, and the bypass flow can be ramped down over an appropriate time to reduce the rate-of-change of flow downstream. If desirable the bypass could be shut down over 30 minutes or more to allow the flow via the gorge to catch up, reducing the downstream flow deficit.

As the flow rate deficit propagates downstream the effect is smoothed out, with rates of change and magnitude of the flow deficit reducing. Comparable model results from a river cross-section a further 2,500 m downstream are shown in Figure 5-2.

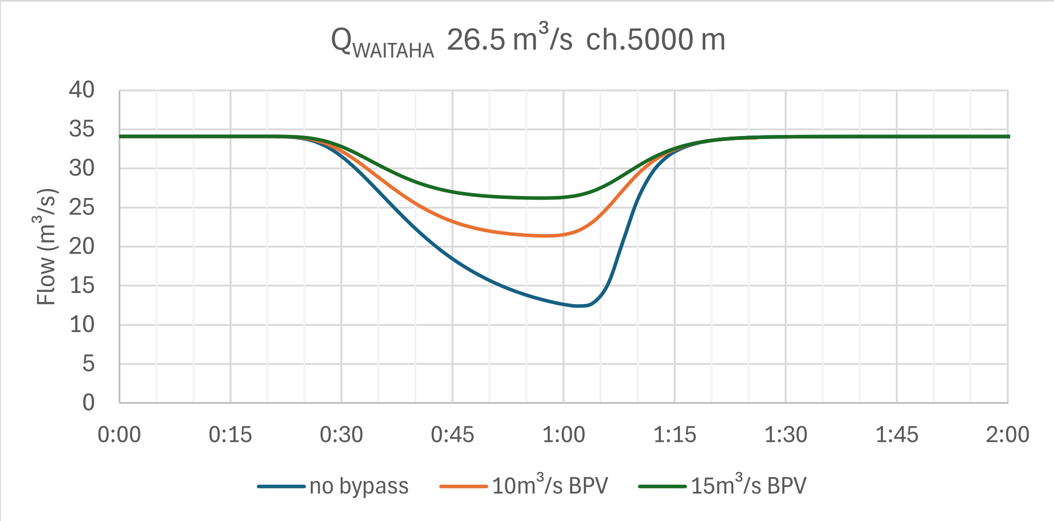

Figure 5-2: Modelled flow in Waitaha River at model chainage 5000m (where braided river reach begins) for three power station flow rejection scenarios, $Q_{WAITAHA}$ = 26.5 m^3/s

5.1.1 Minimum Flowrate

The minimum flow in the Waitaha River following the modelled load rejection scenarios is presented at key locations in Table 5-1 and through the modelled reach in Figures 5-3 to 5-5 below.

Table 5-1: Minimum flow in Waitaha River following load rejection

River Flow $Q_{WAITAHA}$	Power Station	Downstream station	Start of braiding	Model extent
		ch. 2500	ch. 5000	ch. 10000
16.5 m^3/s	*Initial Generation Flow*	17.5 m^3/s	21.3 m^3/s	21.3 m^3/s
	LR - No bypass	4.5	8.9	12.2
	LR -10 m/s BPV	14.5	18.3	18.9
	LR - 15 m/s BPV [a]	17.5	21.3	21.3
26.5 m^3/s	*Initial Generation Flow*	28.2	34.1	34.1
	LR - No bypass	5.1	12.4	18.1
	LR -10 m/s BPV	15.1	21.4	23.8
	LR - 15 m/s BPV	20.2	26.2	27.5

River Flow $Q_{WAITAHA}$	Power Station	Downstream station	Start of braiding	Model extent
		ch. 2500	ch. 5000	ch. 10000
36.5 m^3/s	*Initial Generation Flow*	38.7	47.0	47.0
	LR - No bypass	15.8	25.6	31.3
	LR -10 m/s BPV	25.8	34.6	37.6
	LR - 15 m/s BPV	30.8	39.3	41.1

[a] For a river flow $Q_{WAITAHA}$ = 16.5 m^3/s at the intake, power station discharge is 13 m^3/s, which can all be bypassed through a 15 m^3/s bypass valve, i.e. the minimum flows in this row are the normal river flow ($Q_{WAITAHA}$ plus tributary inflows).

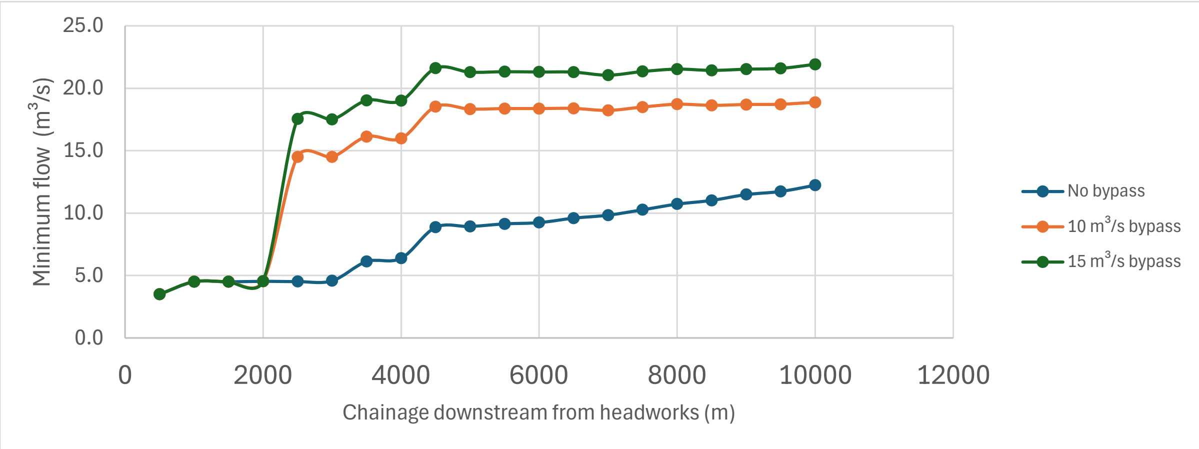

Figure 5-3: Minimum flow in Waitaha River following station load rejection (16.5 m^3/s at headworks), noting that initial flows during station generation at 13 m^3/s are equivalent to the 15 m^3/s bypass valve case.

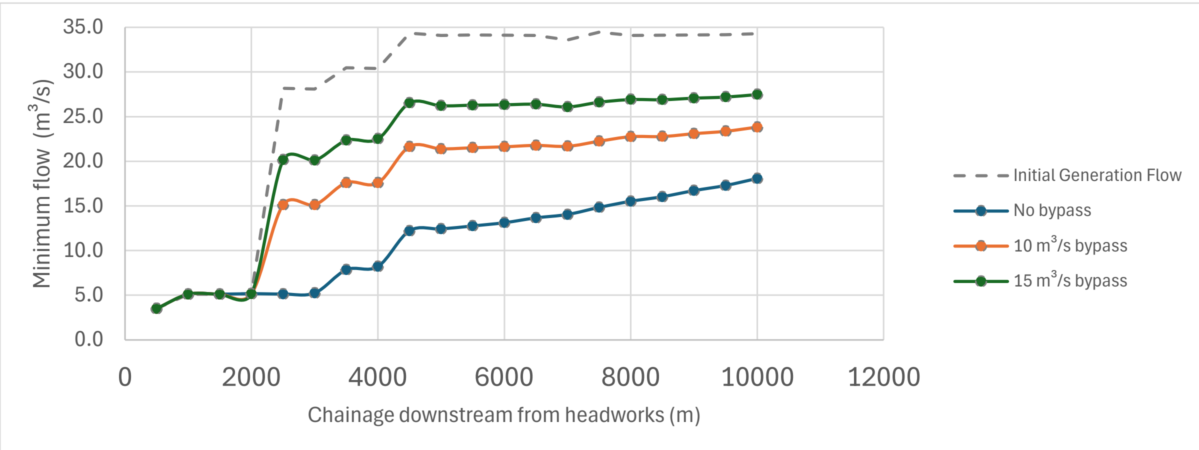

Figure 5-4: Minimum flow in Waitaha River following station load rejection (26.5 m^3/s at headworks)

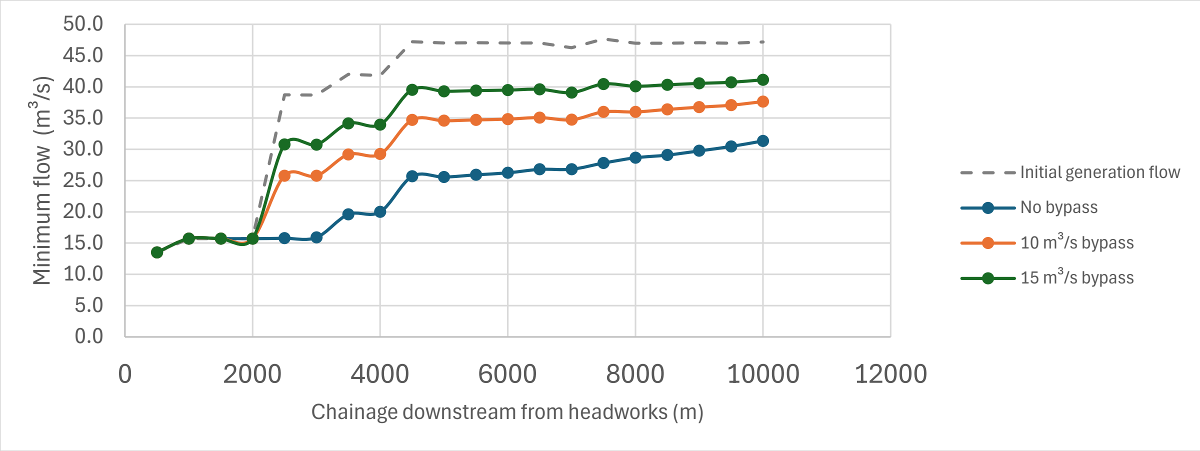

Figure 5-5: Minimum flow in Waitaha River following station load rejection (36.5 m^3/s at headworks)

Minimum flow below the headworks is the minimum residual flow of 3.5 m^3/s for the first two river conditions, increasing downstream due to tributary inflow from Glamour Glen (approx. chainage 1000). Downstream of the power station (ch. 2400), tributary inflows include Douglas Creek (ch. 3300), and MacGregor Creek (ch. 4200).

With distance downstream of MacGregor Creek, the flow deficit is smoothed out, and minimum flow rates gradually increase. This increase in minimum flow (i.e. flattening out of flow deficit) is expected to continue downstream with a flatter river slope and storage within the braided bed, with flow changes becoming imperceptible by the time they reach the coast some 12.5 km further downstream (i.e. ch. 22500).

5.1.2 Time for Flow Recovery

Figures 5-6 to 5-8 show the time following a load rejection event that the river flow is reduced below 50% of the pre-event flow, at different positions along the river. For a station bypass of 10 m^3/s or greater, the downstream flow doesn't drop below 50%. For load rejection with no station bypass, the flow reduction is less than 50% by the downstream end of the model.

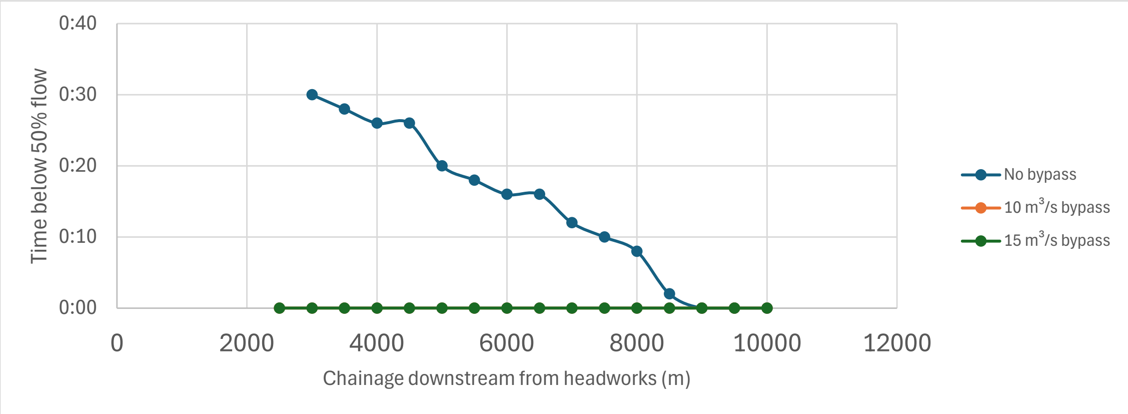

Figure 5-6: Time that river flow is below 50% of pre-event flow (16.5 m^3/s at headworks)

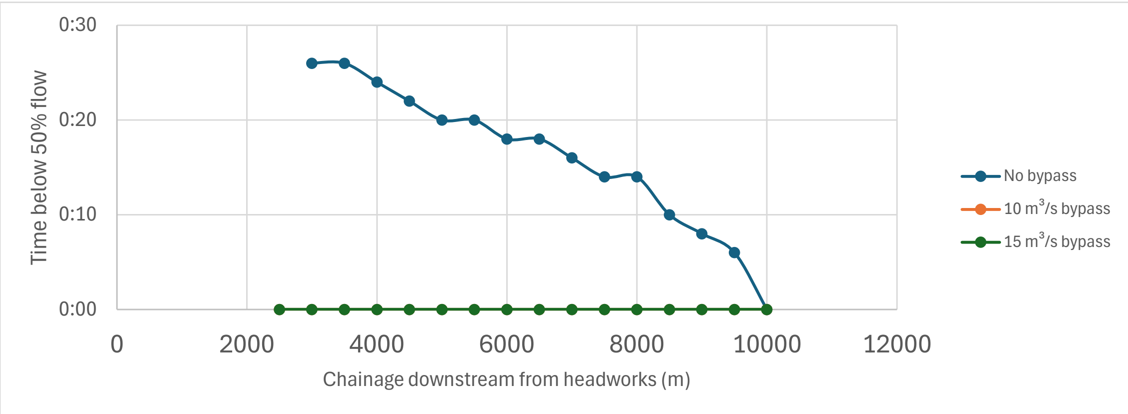

Figure 5-7: Time that river flow is below 50% of pre-event flow (26.5 m^3/s at headworks)

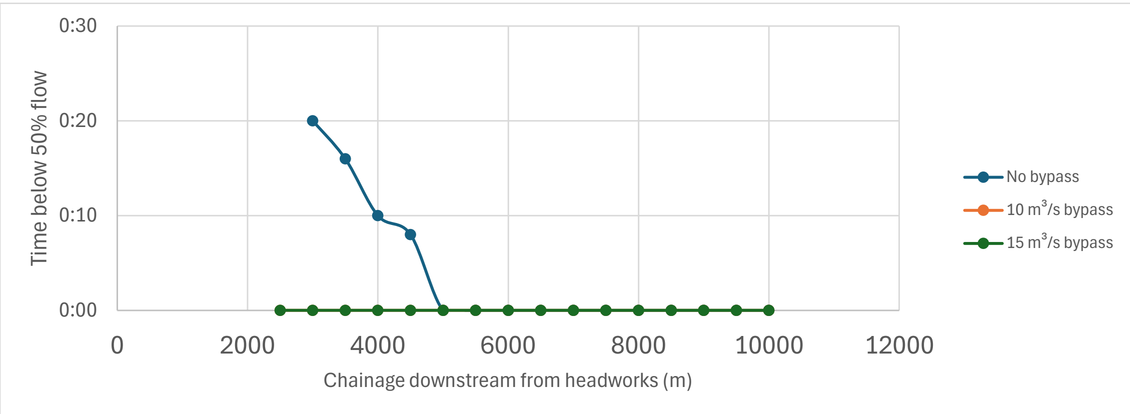

Figure 5-8: Time that river flow is below 50% of pre-event flow (36.5 m^3/s at headworks)

5.1.3 Rate of Change of Flow

The rate of change in flow downstream of the power station following rapid reduction in station outflow is of importance to river users and aquatic fauna. Maximum modelled rates of flow reduction are given in Table 5-2 at key locations. Rates of change of flow reduce with distance downstream, as can be visualised by comparing Figures 5-1 and 5-2 above.

*Table 5-2: Maximum rate of change of flow **reduction** in Waitaha River following load rejection (m^3/s per minute)*

River Flow $Q_{WAITAHA}$	Power Station	Downstream headworks	Downstream station	Start of braiding	Model extent
		ch. 500	ch. 2500	ch. 5000	ch. 10000
16.5 m^3/s	No bypass	0.0 m^3/s/min	2.6 m^3/s/min	0.5 m^3/s/min	0.2 m^3/s/min
	10 m/s BPV	-	0.7	0.2	0.1
	15 m/s BPV	-	-	-	-
26.5 m^3/s	No bypass	-	4.8	1.0	0.5
	10 m/s BPV	-	3.0	0.7	0.4
	15 m/s BPV	-	1.9	0.5	0.2
36.5 m^3/s	No bypass	-	5.1	1.3	0.6
	10 m/s BPV	-	3.1	0.8	0.4
	15 m/s BPV	-	1.9	0.6	0.3

While the rate of change of flow from the turbines is very rapid (23 m^3/s/min for full station flow with no bypass) this change is smoothed out in the river proper (approximately 5 m^3/s/min for the same flow condition at ch 2500 some 100 m downstream) and further reduces as the flow deficit propagates downstream.

Maximum modelled rates of flow increase, as increased flows over the headworks weir arrive, are given in Table 5-3 at key locations. Similarly, these steadily reduce with distance downstream.

*Table 5-3: Maximum rate of change of flow **increase** in Waitaha River following load rejection (m^3/s per minute)*

River Flow $Q_{WAITAHA}$	Power Station	Downstream headworks	Downstream station	Start of braiding	Model extent
		ch. 500	ch. 2500	ch. 5000	ch. 10000
16.5 m^3/s	No bypass	4.3 m^3/s/min	2.5 m^3/s/min	1.4 m^3/s/min	0.5 m^3/s/min
	10 m/s BPV	0.7	0.3	0.2	0.1
	15 m/s BPV	-	-	-	-
26.5 m^3/s	No bypass	6.9	5.2	2.7	0.9
	10 m/s BPV	4.3	2.1	1.1	0.4
	15 m/s BPV	2.6	1.2	0.6	0.3
36.5 m^3/s	No bypass	7.2	4.2	2.2	0.8
	10 m/s BPV	4.2	2.1	1.0	0.4
	15 m/s BPV	2.4	1.1	0.6	0.3

5.2 Controlled Station Shutdown

For a controlled station shutdown there is similarly a drop in river flow before river flow via the gorge increases, but rates of change are significantly decreased compared with station load rejection. A 30 minute station ramp down results in a similar minimum flow as instantaneous shutdown (no bypass scenario in Figure 5-1), while slower shutdowns maintain a higher minimum flow in the river as make-up flow via the gorge arrives before the station flow is completely stopped.

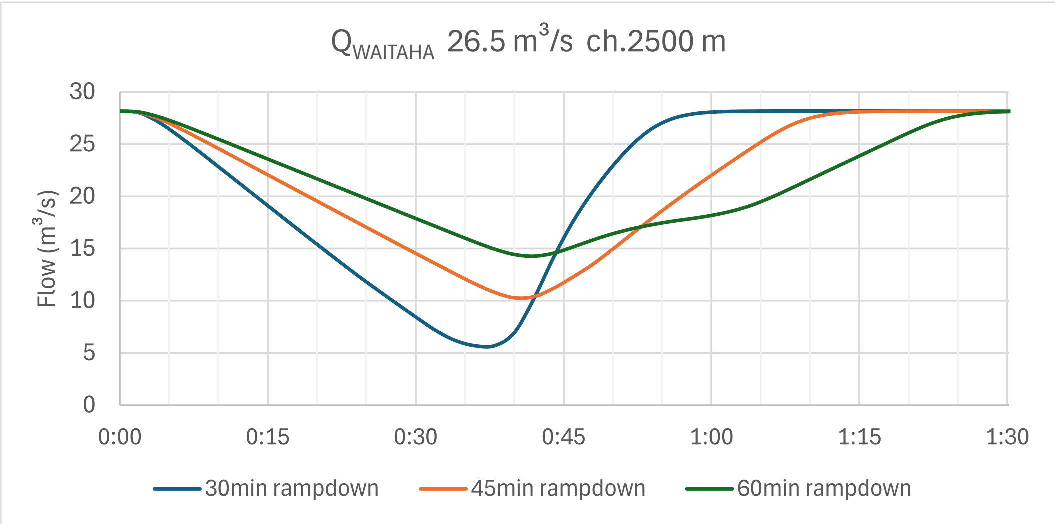

Figure 5-9: Modelled flow in Waitaha River at model chainage 2500 m (100 m downstream of power station) for three power station controlled shutdown scenarios, $Q_{WAITAHA}$ = 26.5 m^3/s

As for load rejection scenarios, the downstream flow deficit is smoothed out with distance downstream, reducing in magnitude as shown in Figure 5-10.

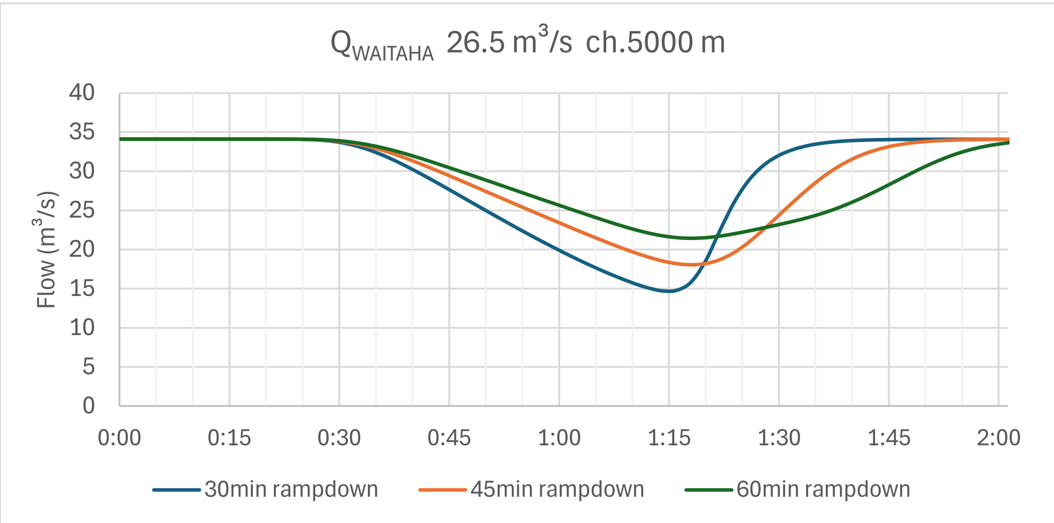

Figure 5-10: Modelled flow in Waitaha River at model chainage 5000m (where braided river reach begins) for three power station flow rampdown scenarios, $Q_{WAITAHA}$ = 26.5 m^3/s

Further results comparable to those presented for load rejection scenarios, including minimum flowrates downstream and rate-of-change of flow are included in Appendix C.

5.3 Station Startup

The temporary increase in river flow rate just downstream of the power station during station startup is shown in Figure 5-11. For a 10 minute station startup, the flow remains elevated for around 15 minutes until the corresponding flow reduction past the headworks propagates down. For a 30 minute station startup, the temporary flow increase begins dropping almost immediately after the station reaches full output.

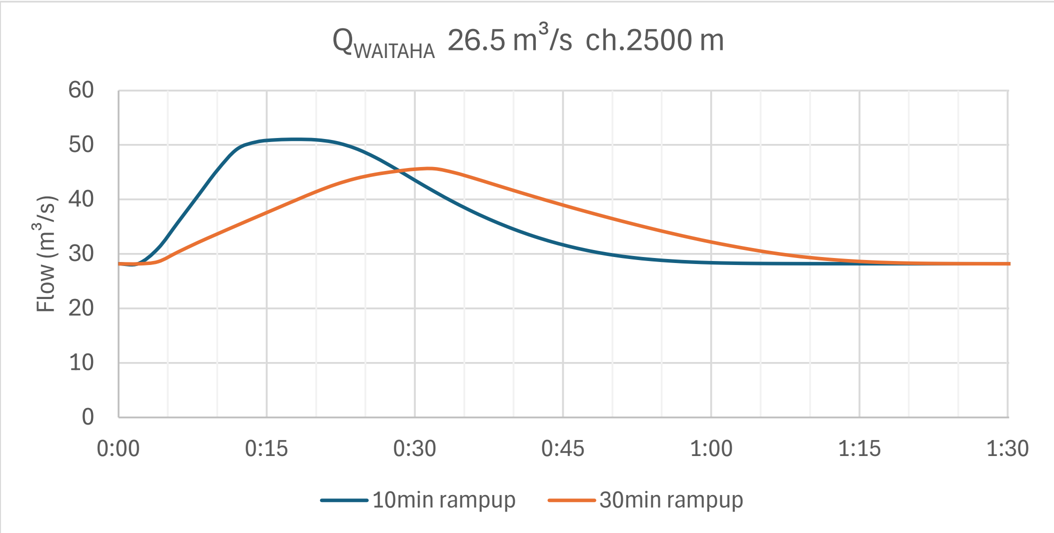

Figure 5-11: Modelled flow in Waitaha River at model chainage 2500m (100 m downstream of power station) during station startup, $Q_{WAITAHA}$ = 26.5 m^3/s

As for the station flow reduction scenarios, the change in flowrate downstream of the station flattens out (reduced magnitude and rates of change) with distance downstream, seen in a comparable plot of flow changes at a cross-section a further 2,500 m downstream (Figure 5-12).

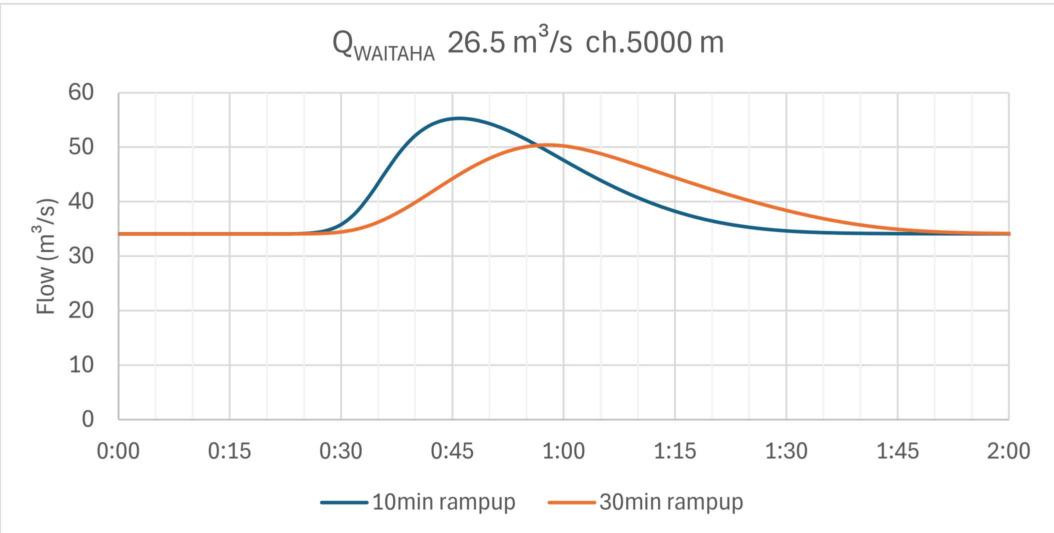

Figure 5-12: Modelled flow in Waitaha River at model chainage 5000m (where braided river reach begins) during station startup, $Q_{WAITAHA}$ = 26.5 m^3/s

For controlled station flow ramp up, the maximum flow in the Waitaha River is presented at key locations in Table 5-4.

Table 5-4: Maximum flow in Waitaha River following power station startup

River Flow Q_{WAITAHA}	Power Station	Downstream headworks	Downstream station	Start of braiding	Model extent
		ch. 500	ch. 2500	ch. 5000	ch. 10000
16.5 m^3/s	*10 min ramp up*	16.5 m^3/s	30.6 m^3/s	33.6 m^3/s	30.7 m^3/s
	30 min ramp up	16.5	29.0	31.6	29.5
26.5 m^3/s	*10 min ramp up*	26.5	51.0	55.3	50.3
	30 min ramp up	26.5	45.7	50.4	47.7
36.5 m^3/s	*10 min ramp up*	36.5	61.6	67.8	62.7
	30 min ramp up	36.5	55.0	62.3	60.0

The increased flow 'pulse' does not substantially flatten as it propagates downstream. Figure 5-13 shows the maximum flow throughout the modelled reach for the two station startup scenarios, showing a very modest decrease in peak flow with distance downstream. Note there are flow increases from tributary inflows at around ch. 3500m (Douglas Creek) and ch. 4500m (MacGregor Creek).

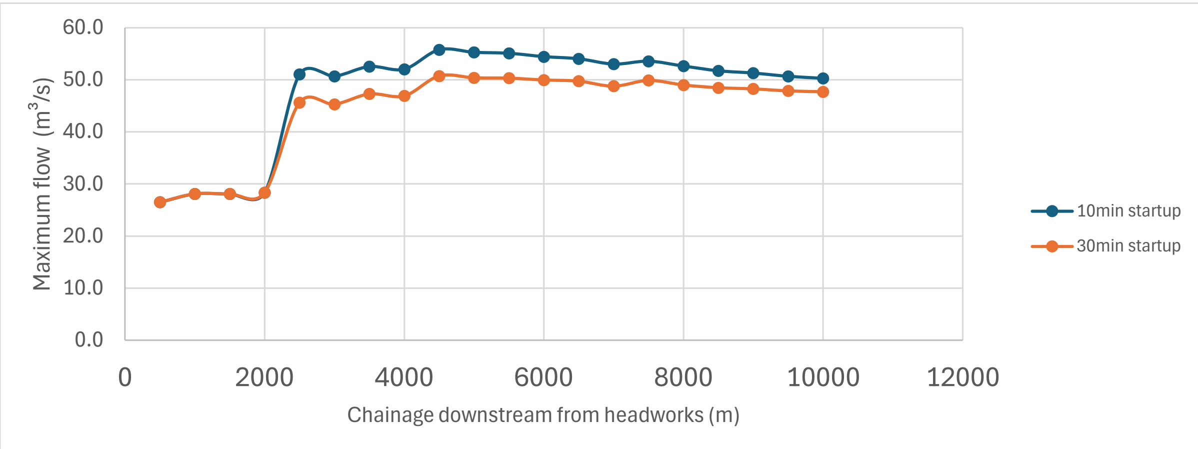

Figure 5-13: Maximum flow in Waitaha River following power station startup (26.5 m^3/s at headworks)

Figure 5-14 plots the maximum rate-of-change of the flow rate increase with distance downstream. Though the peak magnitude of the flow 'pulse' downstream following station startup doesn't reduce appreciably, the maximum rate at which it rises does for the 10 minute startup scenario. For the relatively slow 30 minute station rampup, the rate of rise does not reduce appreciably with distance downstream.

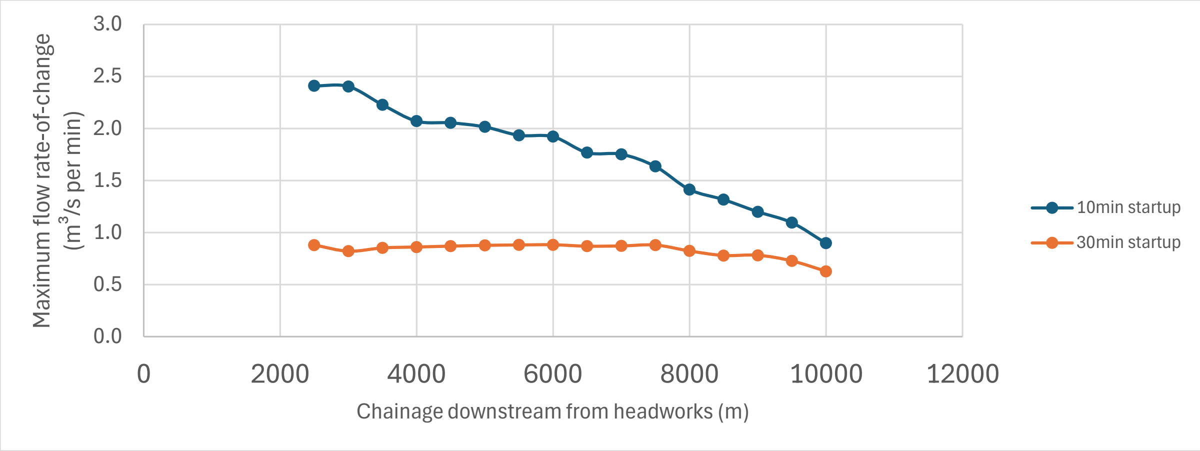

Figure 5-14: Maximum rate-of-change of flow in Waitaha River following power station startup (26.5 m^3/s at headworks)

5.4 Flow Changes at Selected Braided Section

Modelled flow changes in individual braids are presented below across a cross-section at river chainage 7000, in the most braided section of the river. Six main braids are identified, as shown in Figure 5-15.

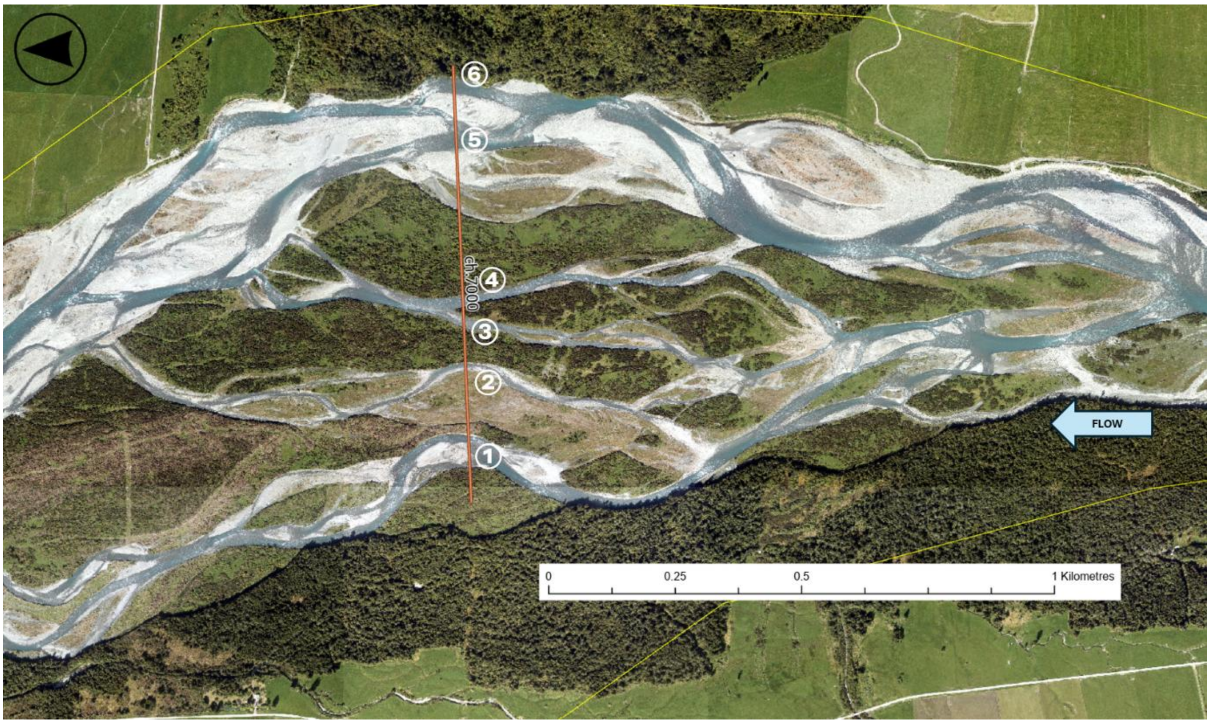

Figure 5-15: River cross-section at chainage 7000m, flow from right to left

The model cross-section is shown in Figure 5-16, with the maximum water surface for the 26.5 m^3/s river condition plotted, along with the minimum water surfaces modelled for scenarios with no bypass and a 10 m^3/s bypass valve.

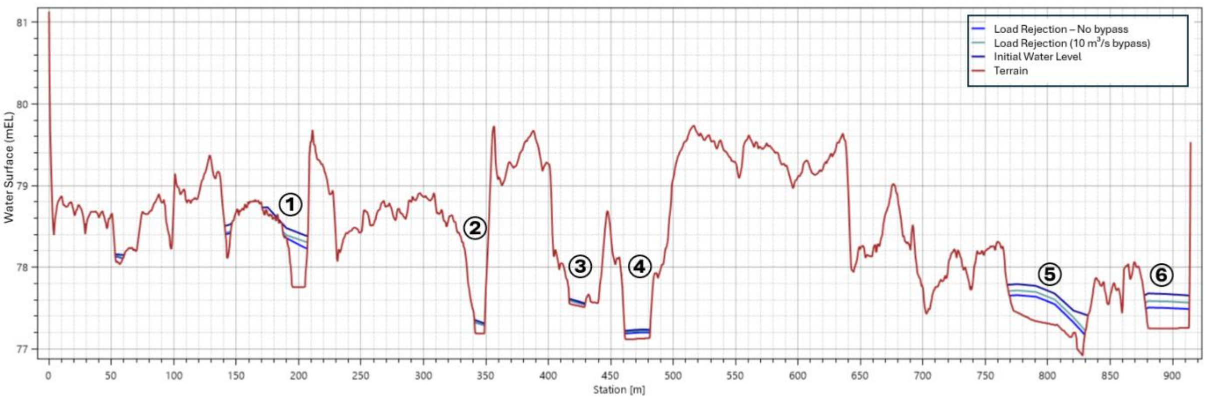

Figure 5-16: Modelled maximum and minimum water surface elevation at ch,7000 for $Q_{WAITAHA}$=26.5 m^3/s, no bypass and 10 m^3/s bypass valve

Flow depths at a point on each braid during steady-state flow, minimum depth following the load rejection scenarios, minimum depth following a 30 minute station shutdown, and maximum depth following a 10 minute station startup are given in Table 5-5.

*Table 5-5: Maximum and minimum **depth (m)** in braids at ch.7000 for $Q_{WAITAHA}$=26.5 m^3/s, for selected station flow scenarios*

Braid	D (pre-event)	D_{MIN} (no bypass)	D_{MIN} (10 m^3/s BPV)	D_{MIN} (15 m^3/s BPV)	D_{MIN} (30min rampdown)	D_{MAX} (10 min rampup)
1	0.61 m	0.46 m	0.53 m	0.56 m	0.48 m	0.70
2	0.18	0.16	0.17	0.17	0.17	0.19
3	0.04	0.03	0.04	0.04	0.03	0.05
4	0.09	0.05	0.07	0.08	0.06	0.11
5	0.41	0.28	0.33	0.36	0.29	0.51
6	0.43	0.25	0.33	0.37	0.28	0.52

For the 26.5 m^3/s river condition, the steady-state flow rates in each braid, minimum flow during the three load rejection scenarios, minimum flow following a 30 minute station rampdown, and maximum flow following a 10 minute station rampup are given in Table 5-6.

*Table 5-6: Maximum and minimum **flow (m^3/s)** in braids at ch.7000 for $Q_{WAITAHA}$=26.5 m^3/s, for selected station flow scenarios*

Braid	Q (pre-event)	Q_{MIN} (no bypass)	Q_{MIN} (10 m^3/s BPV)	Q_{MIN} (15 m^3/s BPV)	Q_{MIN} (30min rampdown)	Q_{MAX} (10 min rampup)
1	9.4 m^3/s	4.9 m^3/s	6.9 m^3/s	7.9 m^3/s	5.5 m^3/s	13.0 m^3/s
2	0.07	0.05	0.05	0.06	0.05	0.08
3	0.13	0.08	0.10	0.11	0.09	0.14
4	0.48	0.20	0.34	0.40	0.23	0.61
5	15.9	6.1	9.8	12.1	7.1	26.8
6	8.0	2.8	4.8	6.0	3.4	12.9

The modelling shows that water levels and flow rates in each braid drop temporarily following the load rejection and station shutdown events, with flow maintained in all braids. Following station startup events, depth and flow temporarily increase in all braids, with the largest increases in the larger right-hand side braid.

It is acknowledged that there is significant uncertainty in results, in particular due to the LiDAR-captured water surface being 'baked-in' to the modelled terrain, and the changeable nature of the riverbed following large flood flows. Regardless, it considered unlikely that significant-sized braids will dry up in the flow reduction scenarios modelled, due to the transient nature of the flow drop which recovers quickly, and the likelihood of subsurface flows through the gravels.

5.5 Change in Flow Depth

Modelled changes in flow depth are presented below at five key locations on the river, identified in Figure 5-17. These include the Morgan Gorge hot spring (ch. 810), downstream of the gorge (ch. 1500), downstream of the power station tailrace (ch. 2500), upstream of the braided reach (ch. 5400) and near the downstream boundary of the model (ch. 10180).

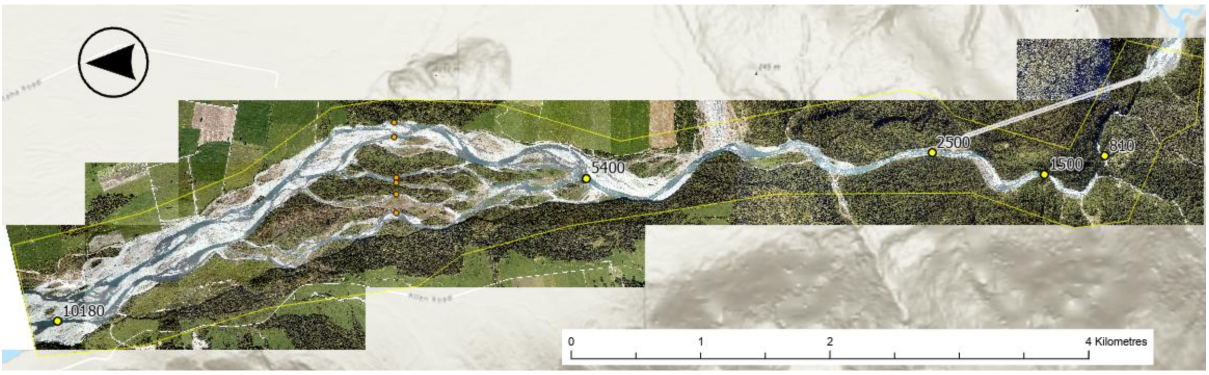

Figure 5-17: Locations where flow depth changes are presented (yellow dots), with position of braids at ch.7000 also highlighted (orange dots).

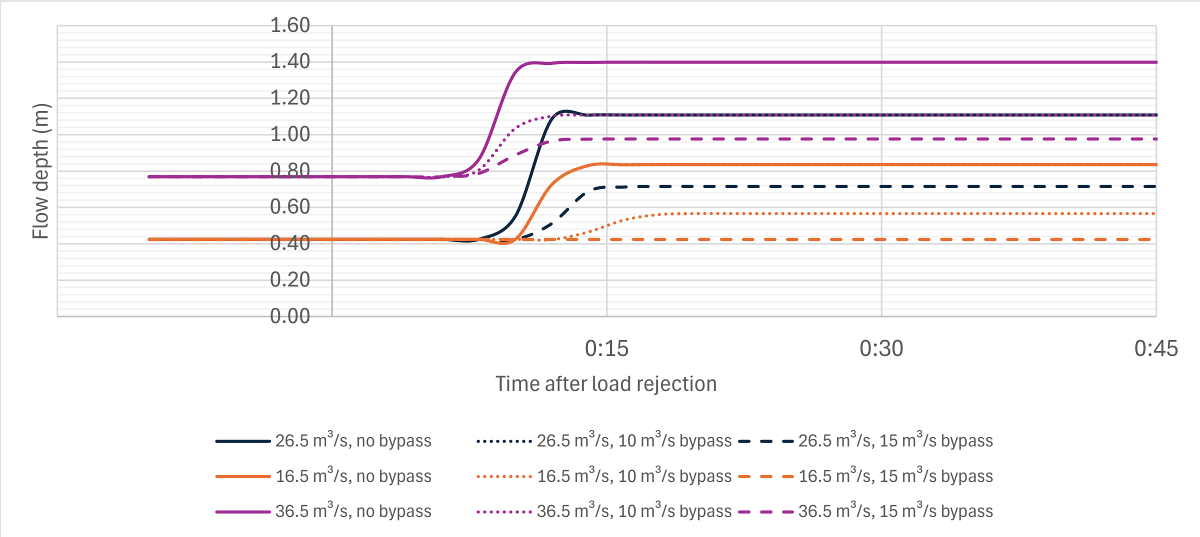

Figure 5-18: Flow depth changes following load rejection at Morgan Gorge hot spring (ch. 810)

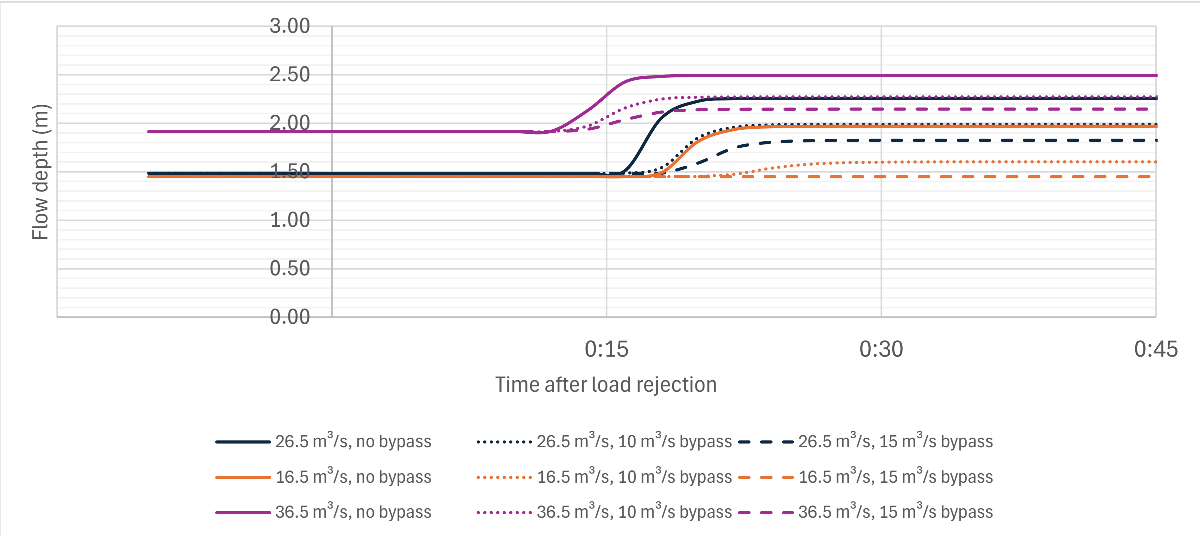

Figure 5-19: Flow depth changes following load rejection downstream of Morgan Gorge (ch. 1500)

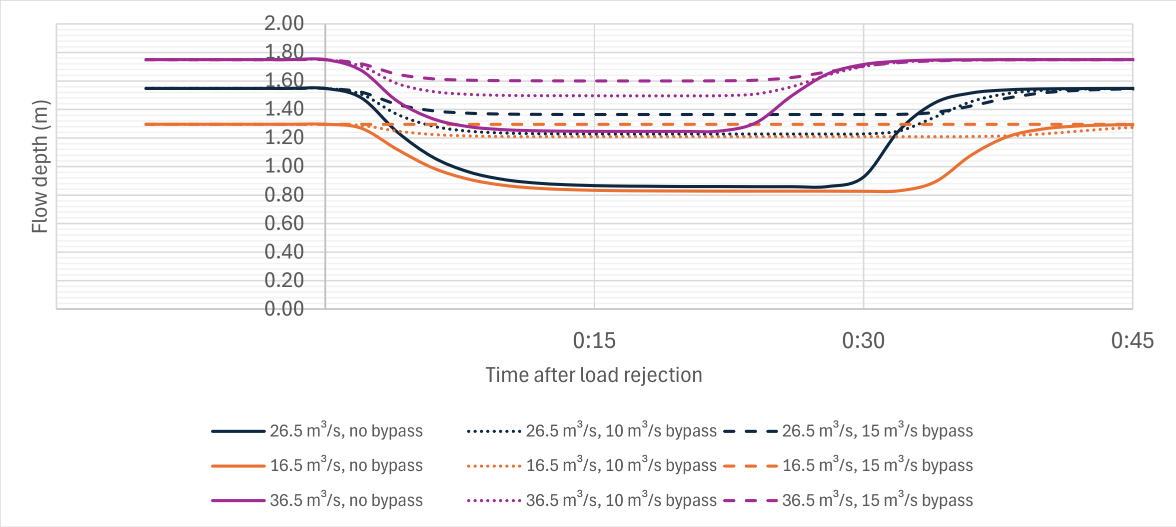

Figure 5-20: Flow depth changes following load rejection downstream of power station (ch. 2500)

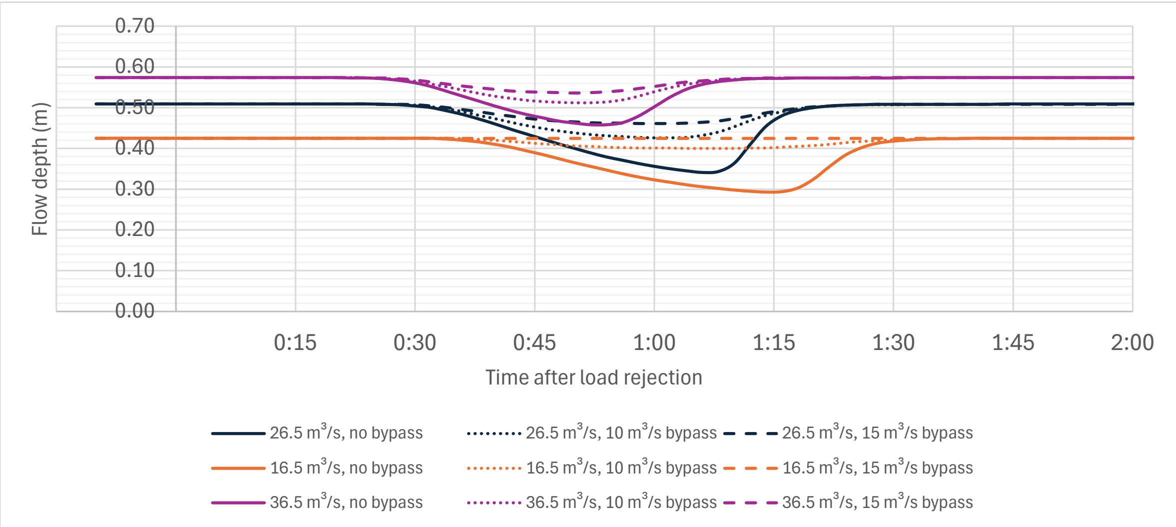

Figure 5-21: Flow depth changes following load rejection upstream of braided reach (ch. 5400)

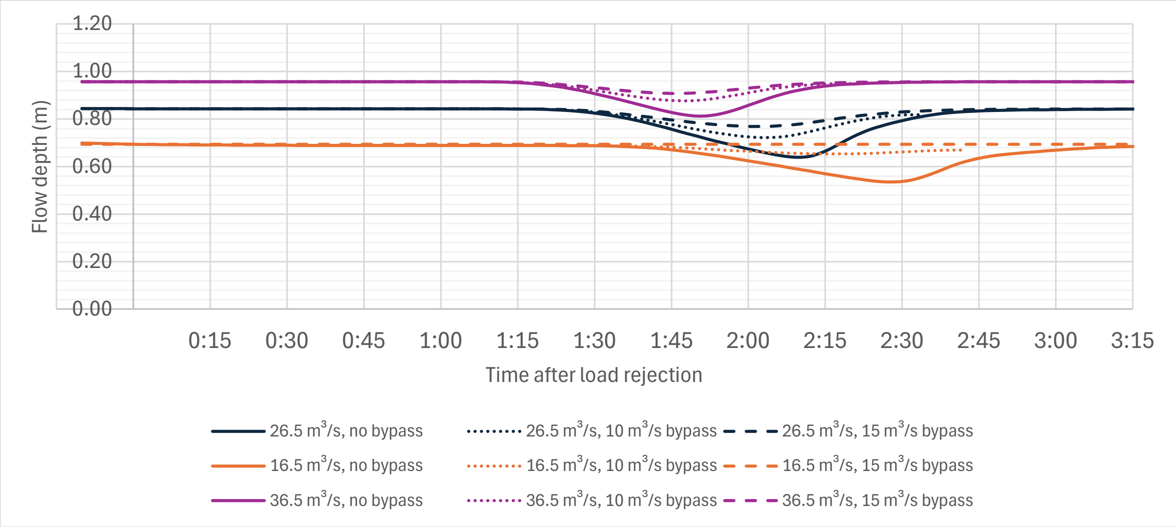

Figure 5-22: Flow depth changes following load rejection near downstream model boundary (ch. 10180)

Following load rejection, the maximum depth within the reach bypassed by the station (experiencing increased flow), and the minimum depth at locations downstream (experiencing temporarily reduced flow) are tabulated below for the three river conditions modelled.

Table 5-7: Steady-state depth mid-channel (before load rejection) and maximum/minimum depth following load rejection for ***$Q_{WAITAHA}$=26.5 m^3/s,*** *no bypass, 10 m^3/s bypass valve, 15 m^3/s bypass valve*

Chainage	D_{STEADY}	D_{MAX} (no bypass)	D_{MAX} (10 m^3/s BPV)	D_{MAX} (15 m^3/s BPV)
810	0.42 m	1.11 m	0.84 m	0.72 m
1500	1.48	2.26	1.99	1.83
		D_{MIN} (no bypass)	D_{MIN} (10 m^3/s BPV)	D_{MIN} (15 m^3/s BPV)
2500	1.55	0.86	1.23	1.37
5400	0.51	0.34	0.43	0.46
10180	0.84	0.64	0.72	0.77

Table 5-8: Steady-state depth mid-channel (before load rejection) and maximum/minimum depth following load rejection for ***$Q_{WAITAHA}$=16.5 m^3/s,*** *no bypass, 10 m^3/s bypass valve, 15 m^3/s bypass valve*

Chainage	D_{STEADY}	D_{MAX} (no bypass)	D_{MAX} (10 m^3/s BPV)	D_{MAX} (15 m^3/s BPV)
810	0.42 m	0.84 m	0.57 m	0.42 m
1500	1.45	1.97	0.60	1.45
		D_{MIN} (no bypass)	D_{MIN} (10 m^3/s BPV)	D_{MIN} (15 m^3/s BPV)
2500	1.30	0.83	1.21	1.30
5400	0.43	0.29	0.40	0.43
10180	0.69	0.55	0.65	0.69

*Table 5-9: Steady-state depth mid-channel (before load rejection) and maximum/minimum depth following load rejection **for $Q_{WAITAHA}$=36.5 m^3/s**, no bypass, 10 m^3/s bypass valve, 15 m^3/s bypass valve*

Chainage	D_{STEADY}	D_{MAX} (no bypass)	D_{MAX} (10 m^3/s BPV)	D_{MAX} (15 m^3/s BPV)
810	0.77 m	1.40 m	1.11 m	0.98 m
1500	1.91	2.49	2.27	2.15
		D_{MIN} (no bypass)	D_{MIN} (10 m^3/s BPV)	D_{MIN} (15 m^3/s BPV)
2500	1.75	1.25	1.50	1.75
5400	0.57	0.46	0.51	0.54
10180	0.96	0.81	0.88	0.91

Equivalent plots and tables for the controlled shutdown and startup cases are included in Appendix D

6 Waitaha Hot Springs and Morgan Gorge

Within the Morgan Gorge reach of the Waitaha River, bypassed by the proposed scheme's waterway tunnel, rapid flow increases following flow reduction at the station may present a safety risk to people within or close to the river. Of particular interest is the hot spring location some 800 m downstream of the diversion weir, which is known to be visited by the public. The hot spring location is elevated above the river during typical flows.

Changes in flow conditions within Morgan Gorge and at the hot spring in particular have been investigated using a revised, more detailed computational model.

6.1 Hot Spring Location

The Waitaha hot spring is a location of particular interest, with publicly available information as to its whereabouts and rough directions to get there [3]. The location is accessed by climbing down the side of the river gorge from the historical walking track on the true left of Waitaha River.

Figure 6-1: Waitaha Hot Spring rock ledge, with bathers showing scale. Photo by Sally Jackson, Wilderness Magazine.

The spring discharges from cracks in the gorge wall onto a rock ledge on the true-left of the river, elevated above the river during typical flows.

[3] E.g. https://nzhotpools.co.nz/hot-pools/waitaha-river-hot-springs/ ; https://leeburty.com/leeburty/2014/02/07/waitaha-river-morgan-gorge-hidden-hot-pool ; https://www.wildernessmag.co.nz/33746-2/

The hot spring was located and visited by Westpower contractors in March 2025, with flow conditions shown in Figure 6-2. On the date of the helicopter flight (11 March 2025) the river flow rate was assessed to be around 8 m^3/s.

Figure 6-2: Hot Spring location (left) from helicopter, (right) from riverbank, March 2025

The spring is at approximate coordinates NZTM 1,415,252 E; 5,222,438 N, some 810 m downstream of the proposed diversion weir following the river centreline.

The location was captured in the 2024 LiDAR survey, as shown in Figure 6-3.

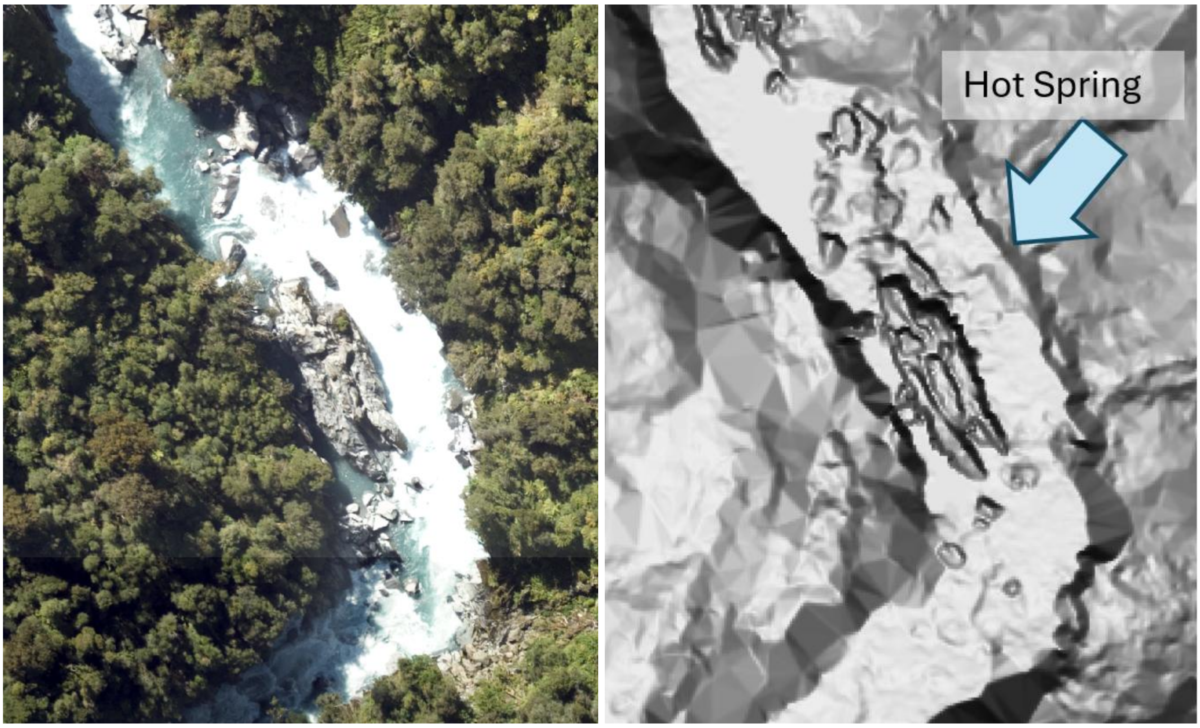

Figure 6-3: Aerial imagery (left) and surface topography (right) from November 2024 LiDAR survey

6.2 Model Approach

A revised model was developed, with a reduced computational domain extending from Kiwi Flat to Glamour Glen, 1 km downstream of the diversion weir. This revised domain has a much finer computational resolution, with flow depth and velocity computed over an unstructured mesh at a maximum spacing of 4 m, reducing to a 1 m mesh for the 150 m river length around the hot spring location.

In this finer-resolution model, computations utilised the shallow water equations (Eulerian Method) which use full momentum terms and accurately capture the associated forces in abrupt contraction and expansion and local flow accelerations due to rapidly changing flow.

The model simulated the load rejection flow scenarios as described in Section 3.

6.3 Water Level vs Flow at Hot Spring

The computational model was run for a range of flow rates to develop a ‘rating curve’ (water surface elevation for given flow rate) at the upstream end of the hot spring rock ledge. From LiDAR, the rock ledge has a surface elevation of around 185.5 to 186.5 m EL. The modelled water surface for river flows of 3.5 m^3/s (proposed minimum flow with Project operating) and 60 m^3/s are shown in Figure 6-4, showing the a significant proportion of the ledge to be inundated at 60 m^3/s or above.

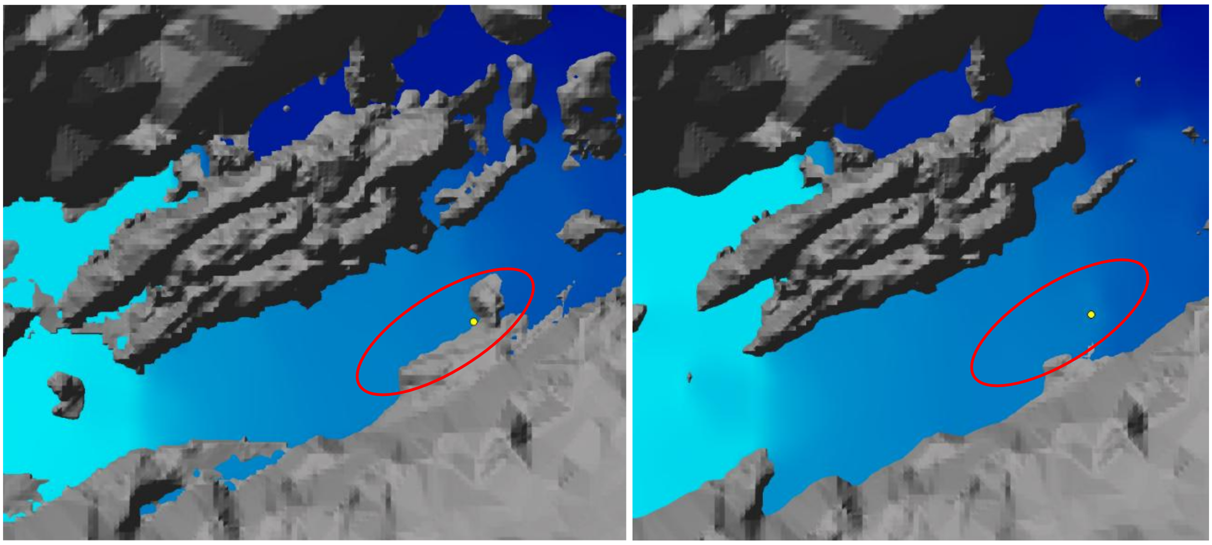

Figure 6-4: Modelled water surface at hot spring location, (left) 3.5m^3/s, (right) 60 m^3/s, with rock ledge indicated

The rating curve at the upstream end of the hot spring rock ledge (at location of yellow dot in Figure 6-4) is given in Figure 6-5, showing that the rock ledge begins to be inundated at a river flow rate of approximately 50 m^3/s, and is submerged 1 m at flows of approximately 100 m^3/s.

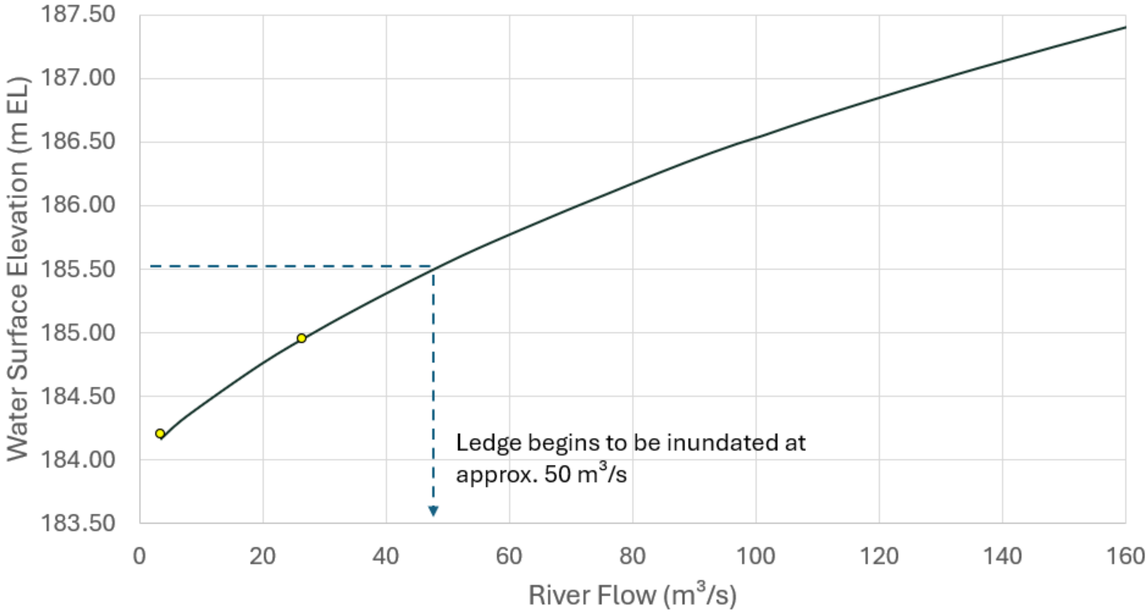

Figure 6-5: Modelled water surface vs river flow at hot spring, with flow conditions before (3.5 m^3/s) and after (26.5 *m^3/s*) load rejection shown as yellow markers

This result is generally consistent with the photograph in Figure 6-1, which shows a relatively low river flow (likely in the order of 15 m^3/s), with the water surface at the upstream end of the ledge around 1 m below the ledge.

The water level rising above the ledge in higher flows concurs with anecdotal evidence that the ledge can sometimes be littered with sediment following large floods.

6.4 Maximum Water Level Rise at Hot Spring Following Load Rejection

The maximum water level rise at the hot spring following a change in station flow will occur at a Kiwi Flat inflow rate of 26.5 m^3/s, as described in Section 3. For this river condition, modelled water surfaces at a cross section at the hot spring location, and a long-section along the river are presented in the figures below, for the three station flow cases.

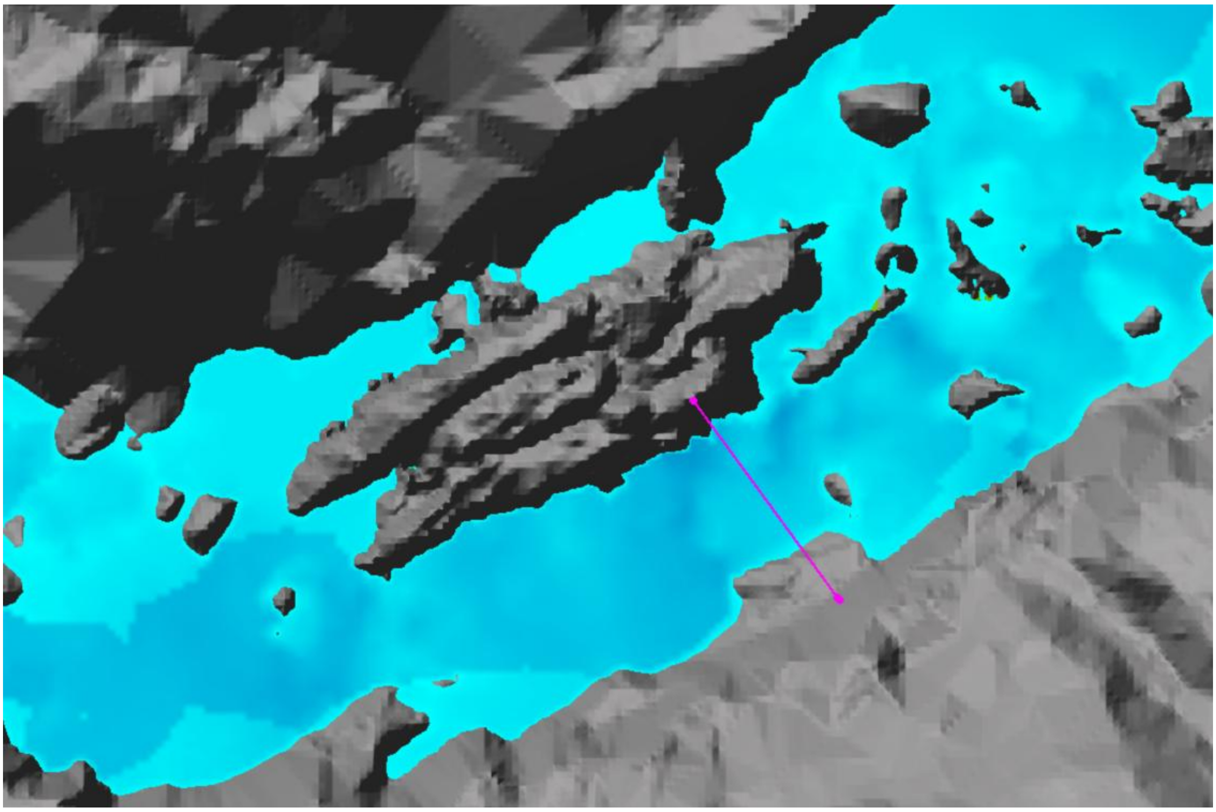

Figure 6-6: River cross-section location at hot spring

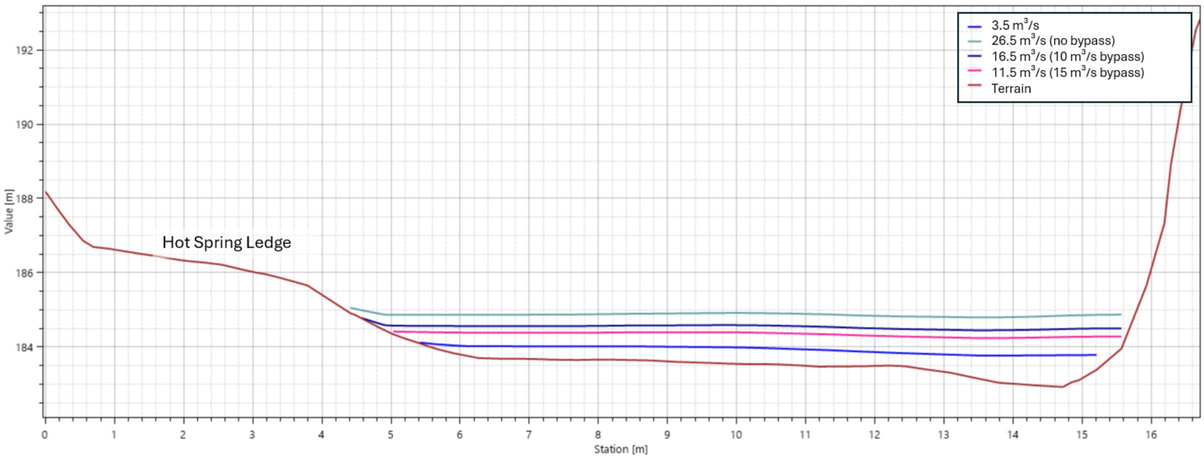

Figure 6-7: Modelled water surface at cross-section

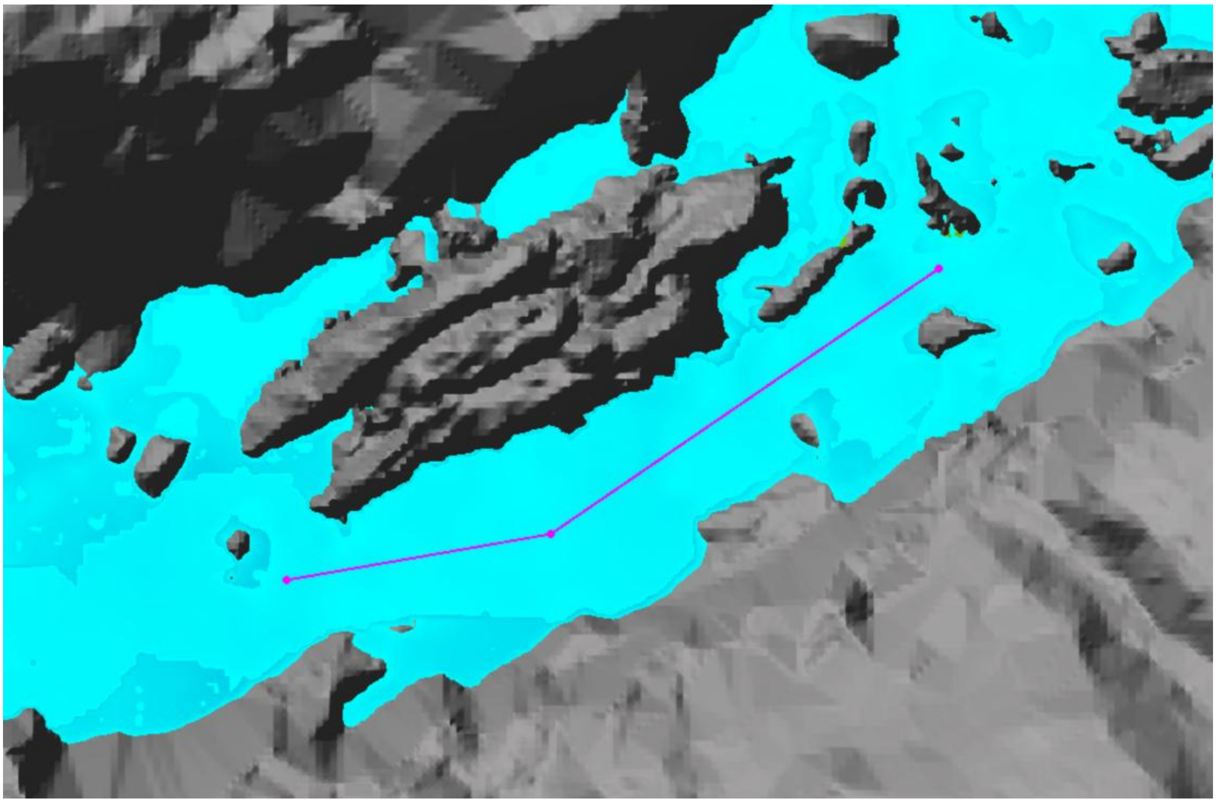

Figure 6-8: River long-section location at hot spring

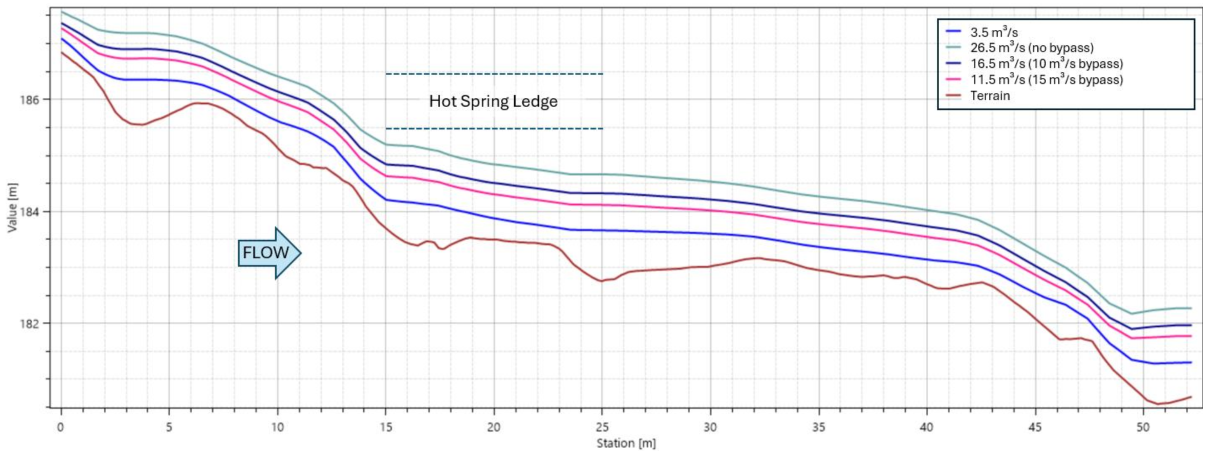

Figure 6-9: Modelled water surface at long-section

These results show that in that in the case with the greatest water level rise following full-station flow rejection, the final water surface is still expected to be well below the level of the hot spring rock ledge. Flow bypass at the station following load rejection significantly reduces the water level increase at the hot spring location.

AusHydro

6.5 Time of Water Level Rise at Hot Spring

A plot of the water level rise with time at the point identified in Figure 6-4 for the three station flow cases is shown in Figure 6-10. For the case with no station bypass, the increase in water level at the hot spring location begins approximately 10 minutes after the station shutdown occurs, and the water level rises approximately 0.75 m over 4 minutes.

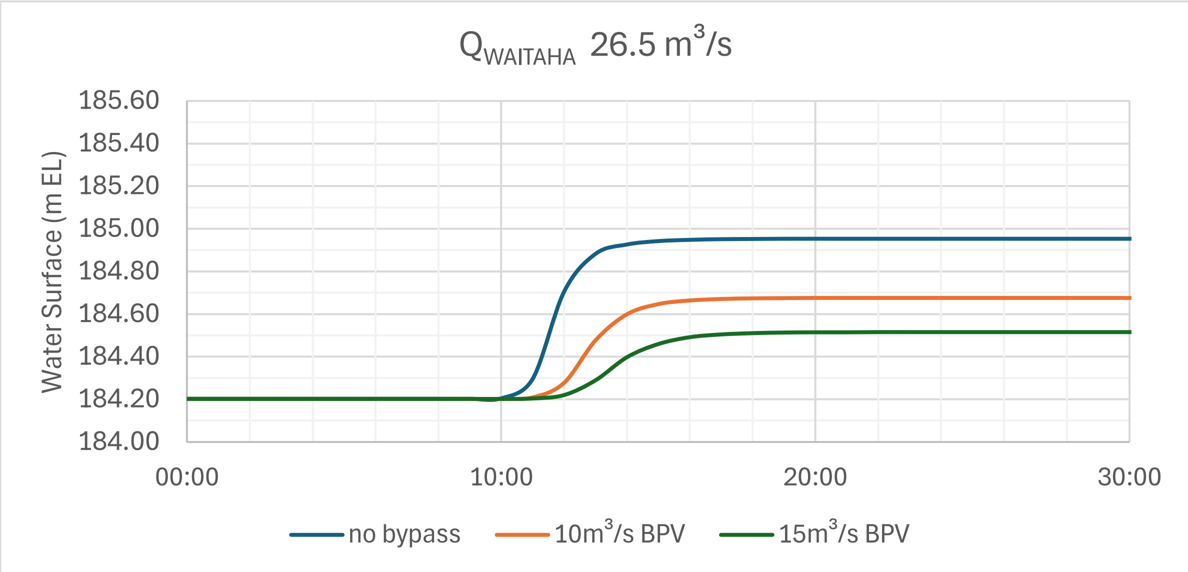

Figure 6-10: Water surface level vs time at hot spring for three station flow cases, $Q_{WAITAHA}$ = 26.5 m^3/s

Similar plots are shown in Figure 6-11 and Figure 6-12 below for lower and higher river conditions.

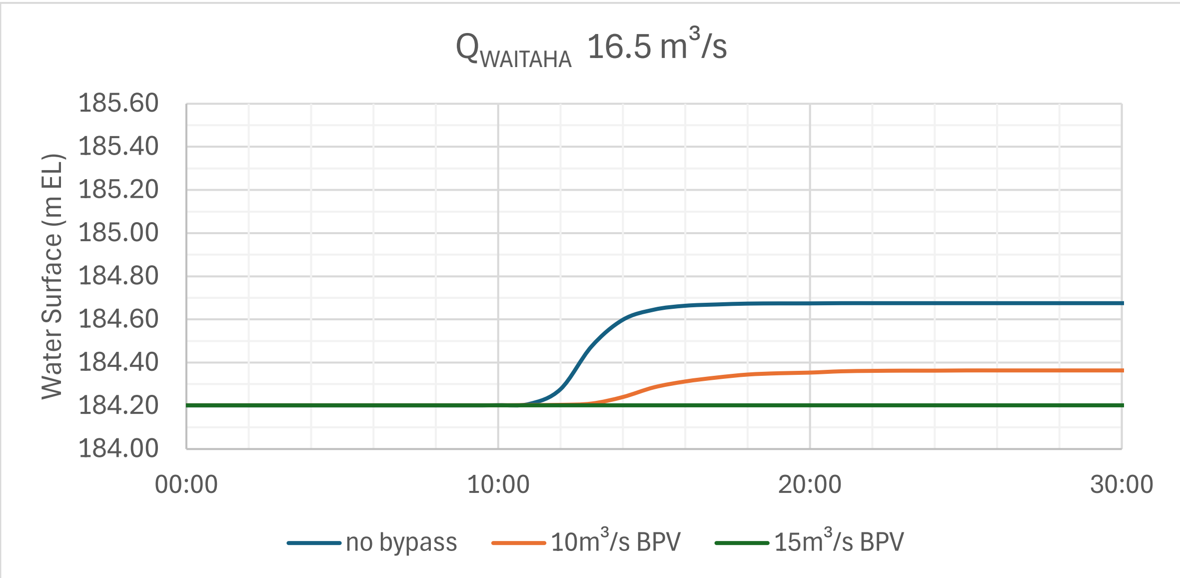

Figure 6-11: Water surface level vs time at hot spring for three station flow cases, $Q_{WAITAHA}$ = 16.5 m^3/s

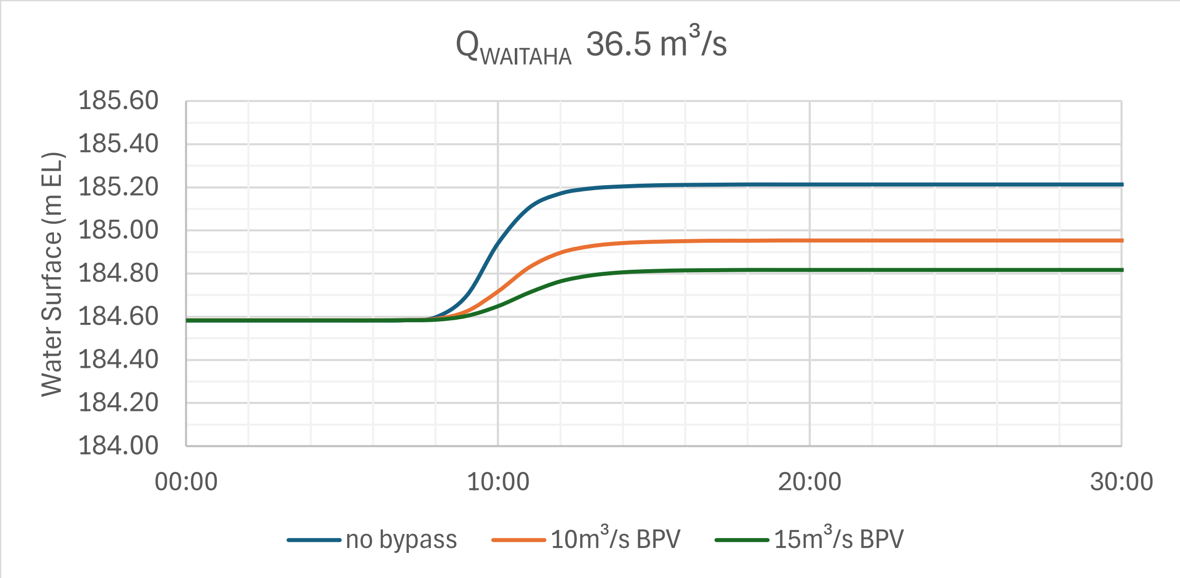

Figure 6-12: Water surface level vs time at hot spring for three station flow cases, $Q_{WAITAHA}$ = 36.5 m^3/s

For these three river conditions, the initial water level (with station operating), the time following station load rejection at which the flow increase arrives at the hot spring location, and maximum water level reached for the three station bypass cases is shown in Table 6-1.

Table 6-1: Initial water surface elevation, time to flood wave arrival and maximum water surface elevation for different river conditions and station bypass cases

River Inflow (m^3/s)	Initial WSL (m EL)	Time to arrival (min)	Max EL no bypass (m EL)	Max EL 10 m^3/s bypass (m EL)	Max EL 15 m^3/s bypass (m EL)
16.5	184.20	11 min	184.68	184.36	184.20
26.5	184.20	10 min	184.95	184.68	184.52
36.5	184.58	8 min	185.21	184.95	184.82

The maximum rise in water depth at the hot spring is 0.75 m without a station bypass valve, reducing to 0.48 m with a 10 m^3/s bypass and 0.32 m with a 15 m^3/s bypass. This occurs around 10 minutes after station load rejection and rises over 4 minutes.

For higher flows in the river, the 'flood wave' of increased flow spilling over the diversion weir travels quicker down the gorge and arrives sooner at the hot spring.

Comparing station load rejection with no bypass for the 26.5 and 36.5 m^3/s river conditions, the difference in water level rise reduces with higher river flows (0.75 m for the 26.5 m^3/s case vs. 0.63 m for the 36.5 m^3/s case).

Extrapolating this out to the condition at which the hot spring ledge begins to becomes inundated (river flow of around 50 m^3/s), the water level rise following full station flow rejection would be in the order of 0.50 m. In the extreme scenario in which people are at the hot spring in high flow conditions with flow lapping at the rock ledge and then full station flow rejection occurs, parts of the ledge would remain above water with a 0.50 m water level rise.

6.6 Flow Rise Hazard at Hot Spring Ledge

The modelling indicates that in the river condition with greatest magnitude of water level rise following load rejection (i.e. 26.5 m^3/s at the headworks), the water level rise will not reach the hot spring ledge.

The worst case for hazard to people at the hot spring will be where the initial water level during station operation is nominally below the ledge (in the order of 42 m^3/s), the highest river condition at which people could reasonably be expected to be there. Full station load rejection from this condition, without bypass valve operation, would cause the flow to rapidly increase to around 65 m^3/s.

The modelled velocities for a flow of 65 m^3/s are shown in Figure 6-13, together with a 0.5 m flow depth contour. The hot spring rock ledge is partially inundated, with velocities of 0 – 2 m/s.

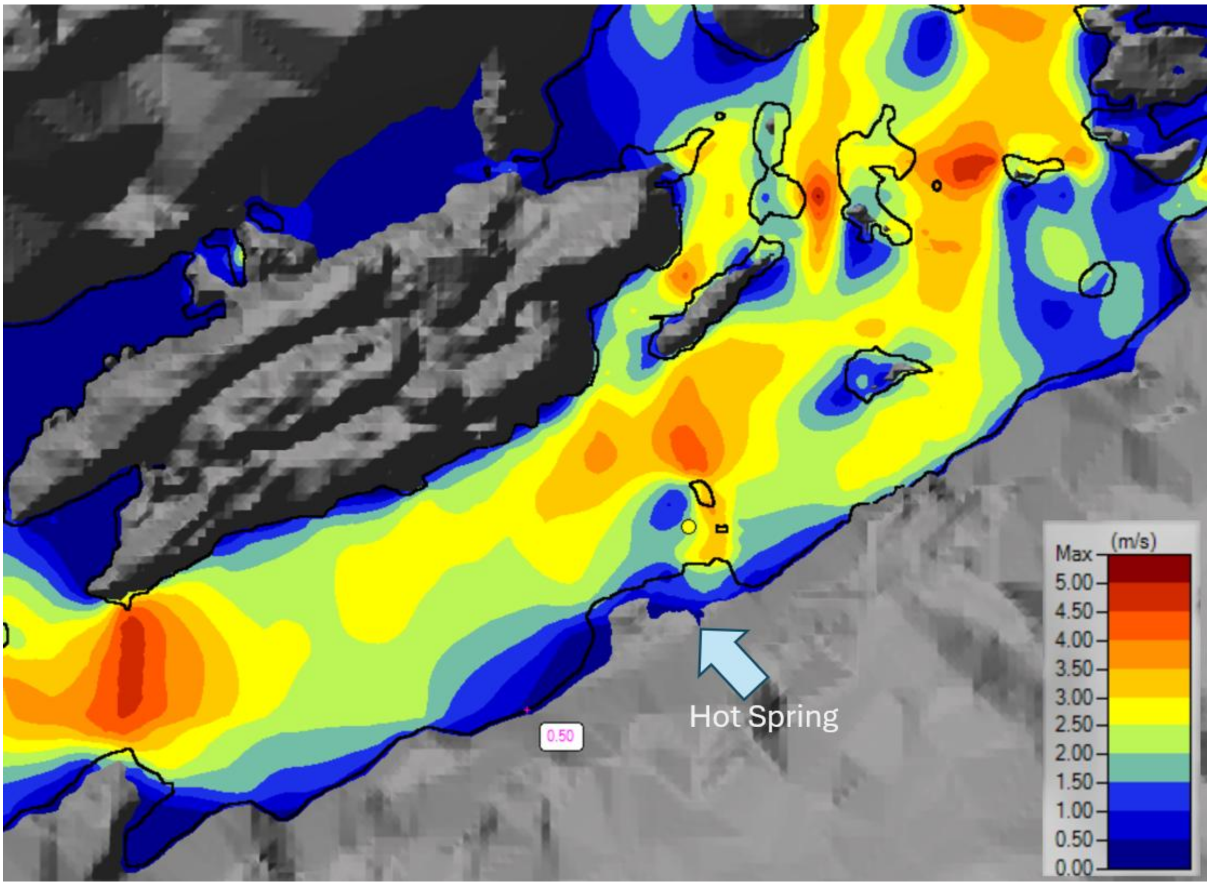

Figure 6-13: Modelled velocities for 65 m^3/s flow near hot spring, with black 0.5m flow depth contour

Flood hazard curves (vulnerability thresholds) are presented by Smith et al. (2014), a hazard assessment methodology widely used by government agencies and industry in both Australia and New Zealand for assessing natural flood hazards (e.g. The New Zealand Dam Safety Guidelines (NZSOLD, 2023)).

The thresholds for people stability in floods presented by Smith et al. (2014), as recommended in *Australian Rainfall and Runoff Revision Project 10: Appropriate Safety Criteria for People*, (Cox, Shand, & Blacka, 2010) are reproduced in Figure 6-14.

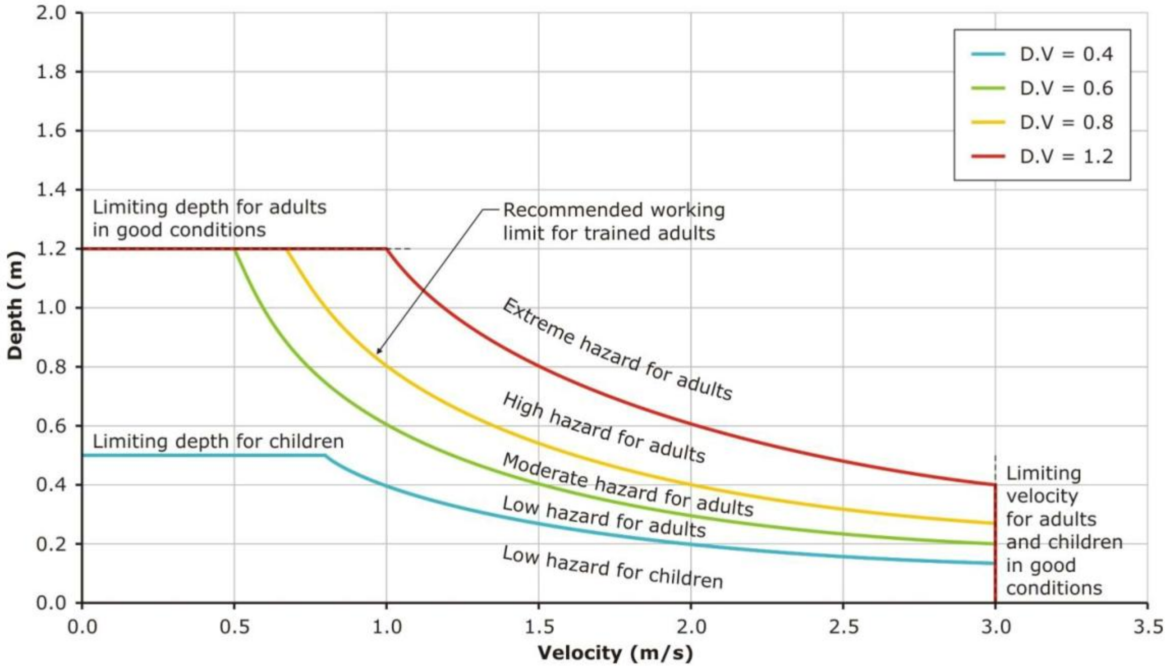

Figure 6-14: Thresholds for people stability in floods (from Smith et al (2014), after Cox et al. (2010)).

The stability curves use DV (depth multiplied by velocity) to delimit different classes of hazard. A DV of less than 0.6 m^2/s is deemed a low hazard for adults if velocities are below 3 m/s.

Considering the worst-case where a full station load rejection occurs with river flow of 42 m^3/s, rising to 65 m^3/s over 4 minutes, modelled DV is shown in Figure 6-15 (with the original flow extent masked). Water rises onto the hot spring ledge, with maximum DV around 0.2-0.4, and velocities are less than 2 m/s (from Figure 6-13). This is considered a low hazard.

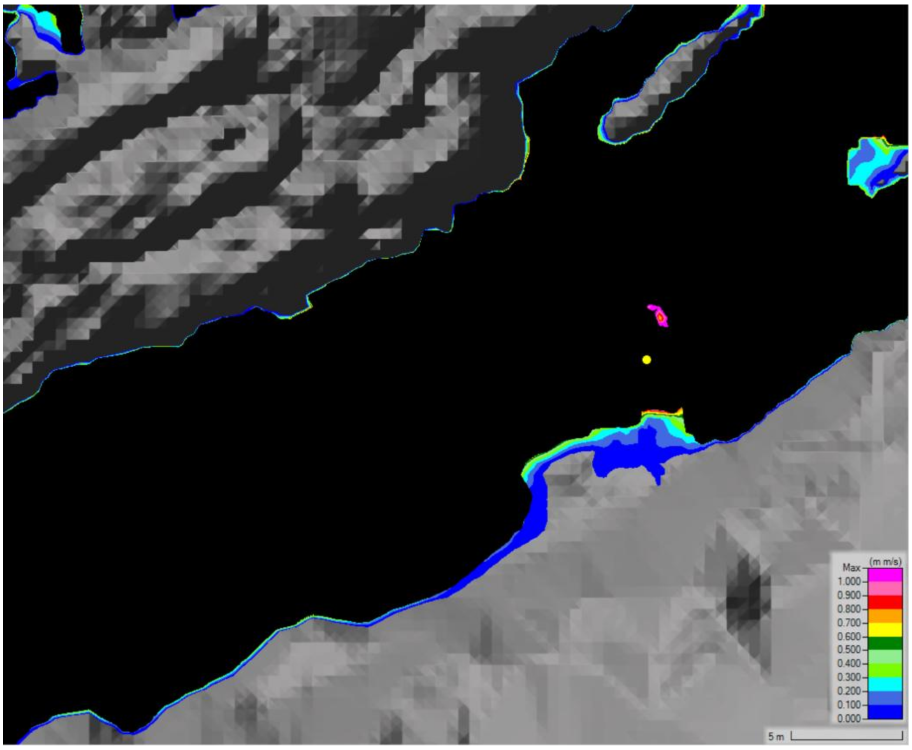

Figure 6-15: DV at hot spring with 65 m^3/s river flow. Black mask covers river extent at 42 m^3/s.

For the same river condition and load rejection but with a 10 m^3/s station bypass, the rock ledge is partially inundated with DV generally less than 0.2 (Figure 6-16).

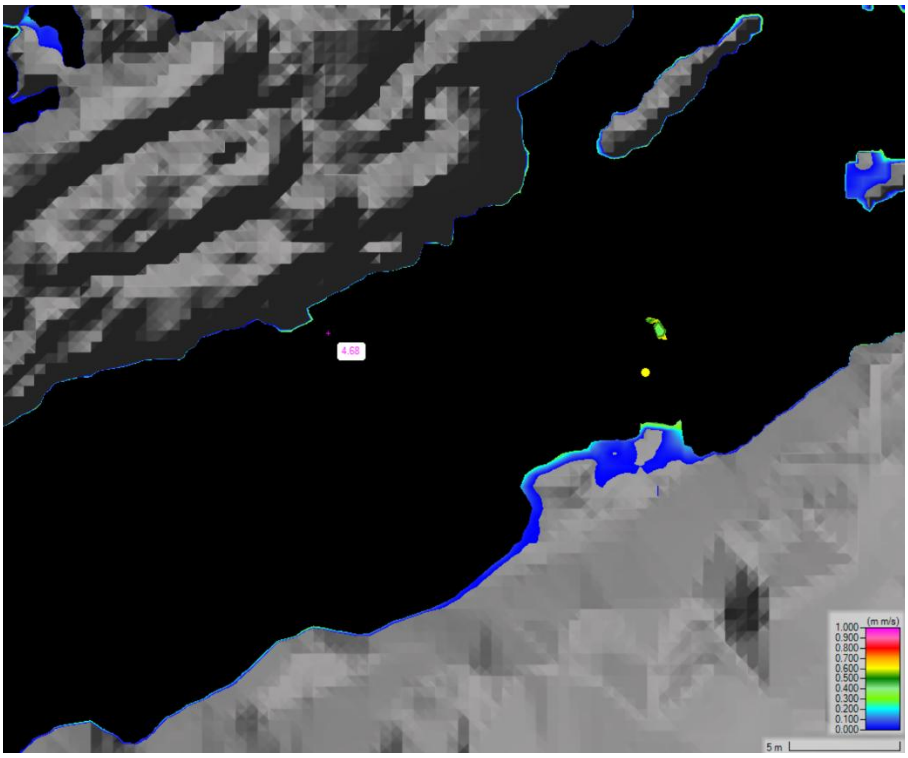

Figure 6-16: DV at hot spring with 55 m^3/s river flow. Black mask covers river extent at 42 m^3/s.

Based on the modelled velocities and depth, flow conditions on the hot spring ledge in the load rejection scenario investigated produce a low hazard, even without a bypass valve operating. In addition, part of the rock ledge remains above water, providing potential for refuge and egress. It must be stressed that this doesn't mean there is zero risk to people at the hot spring, especially with natural hazards, and the swift flowing river immediately beside the ledge.

6.7 Flow Hazard Through Gorge

For the 26.5 m^3/s river condition, a moderate flow hazard following load rejection is indicated by areas where DV is above and below 0.6 m^2/s in Figure 6-17. The location of the hot spring is indicated. This figure shows that the minimum residual flow occupies the full gorge width in many places due to the generally very steep-sided gorge. Following load rejection, there are scattered areas through the gorge which become inundated, with a number of discrete areas of 'moderate hazard' (DV > 0.6).

A comparable plot is shown in Figure 6-18 for the same river condition in which a 10 m^3/s bypass valve is operated following load rejection. In this scenario, very few initially dry areas become inundated with a DV above 0.6.

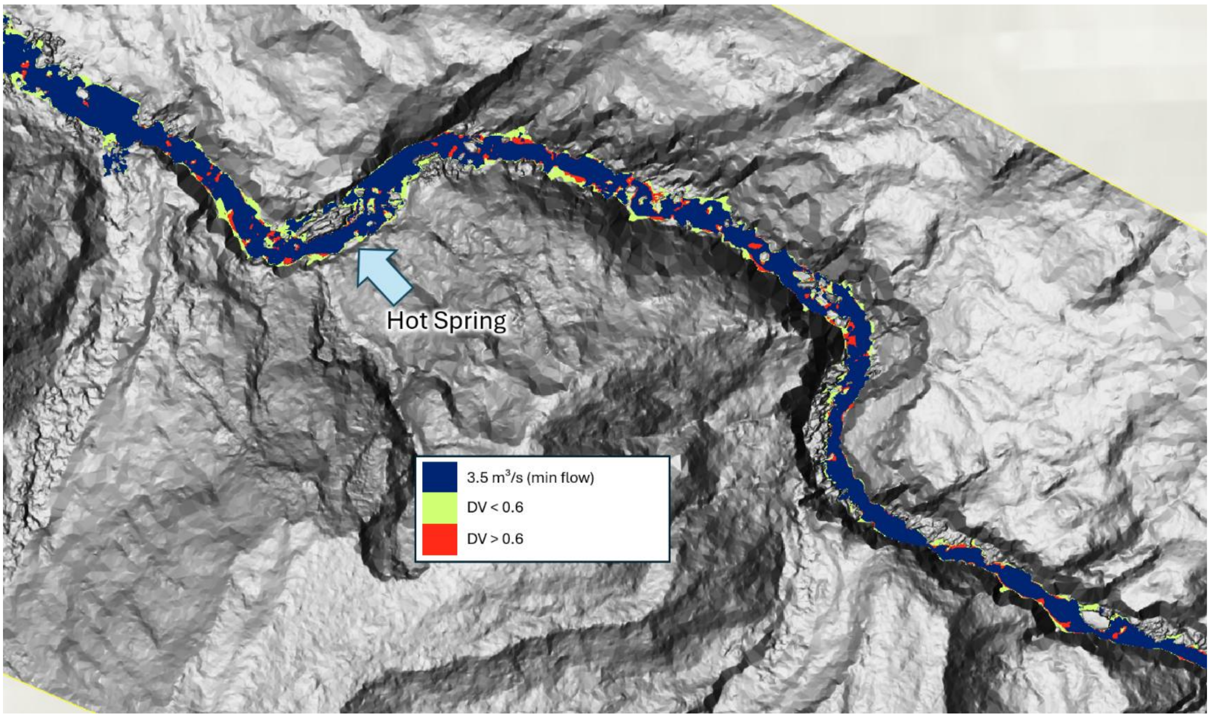

Figure 6-17: Initial flow extent and DV in areas inundated following station load rejection with no bypass $Q_{WAITAHA}$=26.5 m^3/s

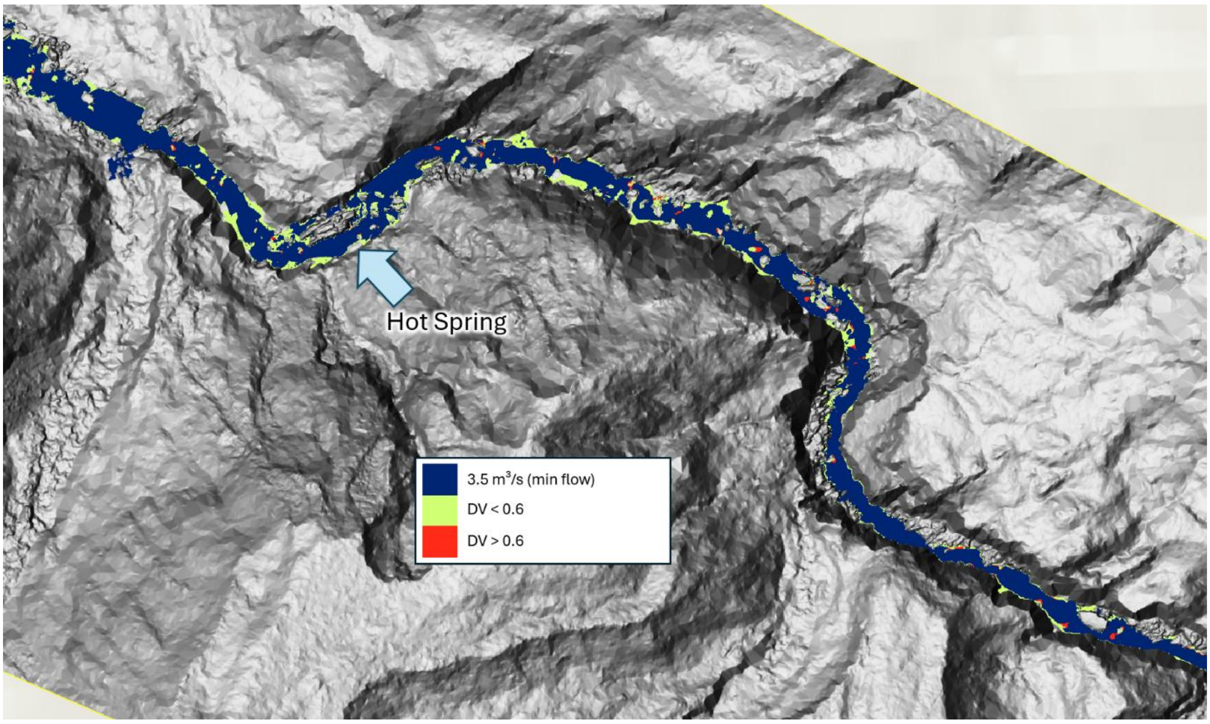

Figure 6-18: Initial flow extent and DV in areas inundated following station load rejection with 10 m^3/s bypass $Q_{WAITAHA}$=26.5 m^3/s

6.8 Need for Bypass Valve

A bypass valve maintains some flow continuity from the power station following load rejection. This reduces the flow deficit downstream, and reduces the flow increase within the bypassed gorge reach. Reducing these rapid flow changes will reduce effects on aquatic fauna and reduce potential safety risks for people on or near the river.

Table 6-2 compares flow hazards within the gorge assessed from the modelling, for load rejection scenarios with and without station bypass.

Table 6-2: Comparison between Morgan Gorge flow hazards following load rejection with no bypass and with 10 or 15 m^3/s bypass

	No Bypass	10 m^3/s Bypass	15 m^3/s Bypass
Maximum WL rise at hot spring	0.75 m	0.48 m	0.32 m
Area of moderate hazard on hot spring ledge	Minimal	None	None
Areas of moderate hazard within gorge	Small	Minimal	Minimal

From a public safety perspective, the model results show that load rejection with no bypass results in moderate hazard levels at only small discrete areas within the gorge, and that the hazard at the hot spring location is generally low. Considering the sporadic presence of itinerant population within the gorge, concentrated mainly at the hot spring, and the low joint probability of occupation coinciding with a load rejection event, the public safety risk in a load rejection scenario even with no bypass is probably very low.

However, given the uncalibrated nature of the model, and known limitations in the modelled terrain, model outcomes should be applied with conservatism, and the low (but slightly uncertain) flood hazard level can be appropriately managed by allowing for a 10 m^3/s bypass valve in the power station design.

If desired, further field data collection could be undertaken to allow more precise modelling and confirm the need for a bypass valve. Data would include flow records and water level measurements to allow model calibration and verification, detailed survey of the rock ledge, adjacent river bathymetry, and egress route, and quantification of public presence at the hot spring and within the gorge.

7 Conclusions

2D computational hydraulic modelling was undertaken to investigate the response of Waitaha River flows following rapid changes of discharge from the power station, including load rejection (i.e. sudden loss of power generation) and station startup and shutdown.

The model terrain was based on LiDAR topographic data captured in November 2024. The topography does not accurately reflect the riverbed elevations below the water-surface on the day of data capture, and thus results are indicative as opposed to precise, and appropriate conservatism should be used when applying model outcomes.

Eight operational scenarios were accessed, reflecting load rejection/acceptance cases and operational scenarios using variable ramp rates and bypass valves to control the rate of flow change. The hydraulic effect of each of these scenarios were reviewed at two main locations:

- Downstream of the power station in braided reaches. This modelled reach extended some 7.5 km downstream of the station and was assessed to understand flow change and potential for adverse ecological impacts such as fish stranding.
- Within Morgan Gorge, in particular at the hot spring location approximately 800 m downstream of the proposed diversion weir. The purpose was to assess potential water level change, travel times and associated flood hazard, to aid in understanding the potential public safety impact.

The key findings at both locations were as follows:

Downstream braided reach:

The modelled lag time between load rejection and recovery of the steady-state flow just downstream of the power station ranges from 30 to 40 minutes, during which time there is a reduction in river flowrate and water level. As this temporary flow deficit travels downstream, the water level difference and flow rate changes reduce.

Over the modelled reach, the magnitude of flow reduction drops to be less than 50% of the steady-state flow for all scenarios modelled.

Flow within individual braids at a river section 4.5 km downstream of the station have been assessed. The modelling indicates that water levels and flow rates in each braid drop temporarily following the load rejection events, with flow maintained in all braids.

Modelled changes in flow depth are presented at five key locations on the river, both within and downstream of the reach bypassed by the station. Depth changes throughout the reach are significantly lower in the scenarios with a bypass valve (as expected) due to the smaller change in flow rate.

When slow ramp rates are assessed (e.g. 30-, 45- and 60-minutes ramp-down), depth changes take longer to manifest, and are slightly lower in magnitude than for the scenario with an immediate drop in station flow.

Morgan Gorge and Hot Spring:

The modelling shows that the hot spring rock ledge is expected to start being inundated at natural river flows of around 50 m^3/s. This agrees with anecdotal evidence (i.e. online discussion) describing the appropriate river conditions to access the hot springs. Based on the historical record, flows greater than 50 m^3/s occur about 10% to 15% of the time.

Following the rejection of electrical load at the power station (e.g. loss of transmission line connection) and resulting flow rejection, river inflows will rapidly build up at Kiwi Flat and overtop the diversion weir, increasing flow within the gorge.

The greatest river level rise following load rejection will occur when station flow is maximum (23 m^3/s) and the residual flow in the gorge is minimum (3.5 m^3/s) – a total river inflow rate of 26.5 m^3/s. In this scenario, the modelled water level rise following rejection of the full station flow is approximately 0.75 m at the hot spring location. This surge would not inundate the rock ledge on which the hot spring discharges, given its relatively high elevation. A 10 m^3/s bypass valve operating at the station reduces the modelled water level rise to less than 0.50 m.

At the highest flow rates during which people could reasonably be expected to be at the hot spring, load rejection would lead to inundation of a significant proportion of the rock ledge, with depths up to 0.5m and velocities up to 2 m/s, and the depth-velocity product being generally 0.2-0.4 m^2/s constituting a low hazard for adults following Smith et al (2014).

The flow increase at the hot spring location occurs around 10 minutes after flow rejection at the power station and rises over 4 minutes.

There are small, scattered areas within the gorge which become inundated following load rejection, with a number of small areas of 'moderate hazard' (DV > 0.6) in the no-bypass scenario, but minimal areas with DV above 0.6 for scenarios with a bypass valve operating.

Need for Bypass Valve

A bypass valve maintains some flow continuity from the power station following load rejection. This reduces the flow deficit downstream, and reduces the flow increase within the bypassed gorge reach. Reducing these rapid flow changes will reduce effects on aquatic fauna and reduce potential safety risks for people on or near the river.

The flood hazard within the gorge in a load rejection scenario is low, even with no station bypass, given the elevated setting of the hot spring, relatively low inundation depths and velocities in worst-case conditions, and relatively small areas of hazardous inundation depth/velocity elsewhere in the gorge. With an expected low joint probability of the presence of people coinciding with a load rejection event, the associated public safety risk is probably very low. However, given the uncalibrated basis of the model, and known limitations in the modelled terrain, model outcomes should be applied with conservatism. The low (but slightly uncertain) flood hazard level can be appropriately managed by allowing for a 10 m^3/s bypass valve in the power station design.

7.1 Recommendations

It is recommended that the environmental effects and personnel safety risk of rapid power station flow changes are assessed based on the indicative information provided in this report.

Based on a conservative consideration of the modelling outcomes, it is recommended that allowance for a 10 m^3/s bypass valve is included in the power station design.

If desired, further field data collection could be undertaken to allow more precise modelling and confirm the need for a bypass valve. Data would include installation of a flow gauging station and collection of water level records to allow model calibration and verification, detailed survey of the rock ledge, adjacent river bathymetry, and egress route, and quantification of public presence at the hot spring and within the gorge.

It is recommended that appropriate public safety warnings and/or signage are planned to alert visitors to the potential hazard of rapidly increasing flow within the gorge.

8 References

Cox, R. J., Shand, T. D., & Blacka, M. J. (2010). *Australian Rainfall and Runoff Revision Project 10: Appropriate Safety Criteria for People*. Water Research Laboratory. P10/S1/006.: Australian Rainfall and Runoff Revision .

Hicks, D. M., & Mason, P. D. (1998). *Roughness Characteristics of New Zealand Rivers*.

Jarrett, R. D. (1984). Hydraulics of High-Gradient Streams. *Journal of Hydraulic Engineering*.

NZSOLD. (2023). *New Zealand Dam Safety Guidelines*.

Smith, G. P., Davey, E. K., & Cox, R. J. (2014). *Flood Hazard*. *WRL Technical Report 2014/07*. University of New South Wales Water Research Laboratory.

Appendix A –Photographs of Gravel-Bed Rivers for Assessment of Appropriate Model Roughness

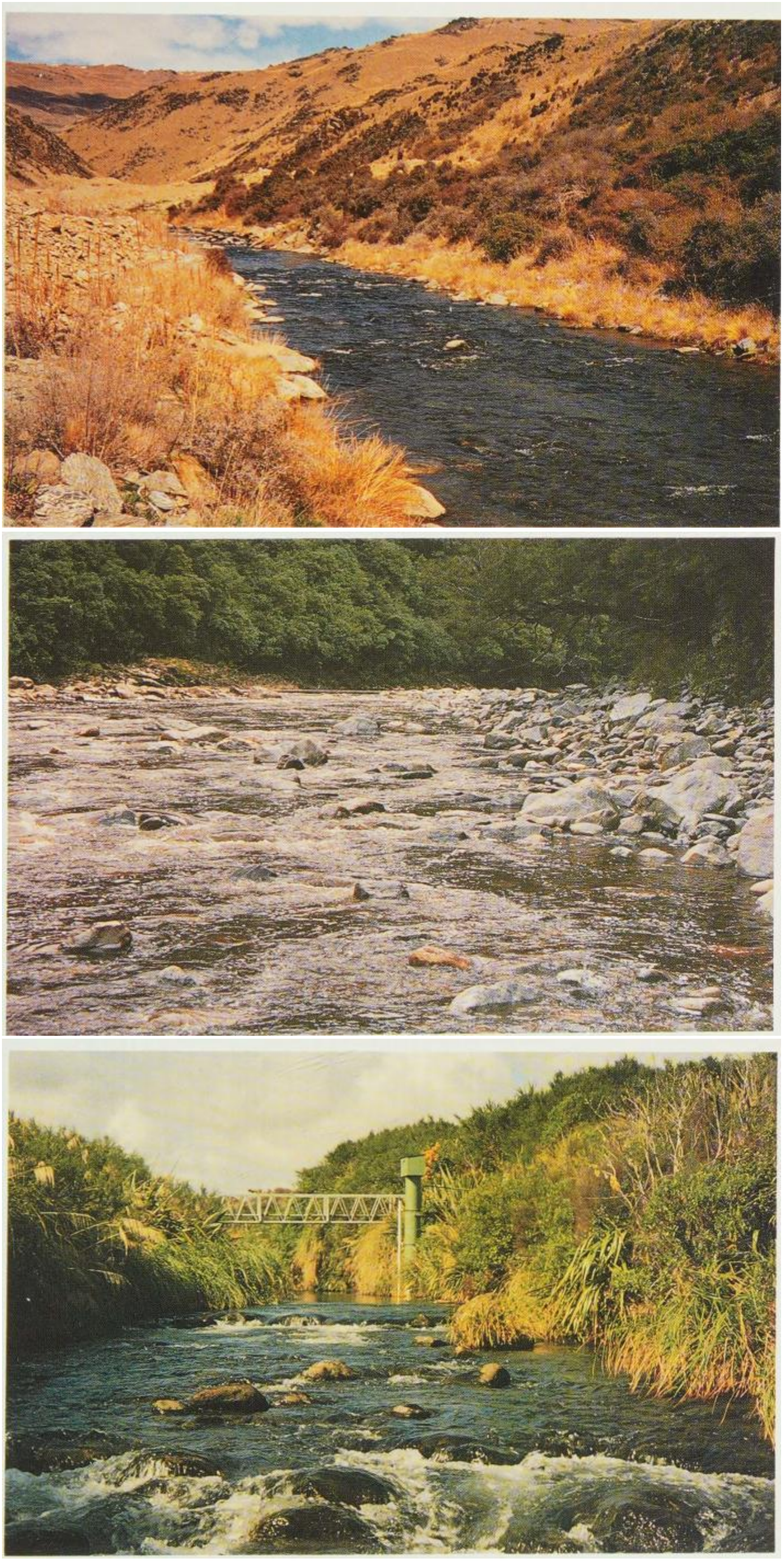

Figure A-1: Examples of boulder/gravel-dominated bed roughness – (top) Cobb at Old Man Range, n=0.061 (middle) Ngakawau at Lineslip, n=0.088 (bottom) Wanganui at Te Porere, n=0.16 (Hicks and Mason, 1998)

Figure A-2: Waitaha River within Morgan Gorge, approx. ch. 500 (source: leeburty.com)

Figure A-3: Waitaha River at approx ch. 3000 looking upstream (29 Feb 2024)

Figure A-4: Waitaha River at approx ch. 6000 looking upstream (29 Feb 2024)

Appendix B –Sensitivity to Roughness Assumptions

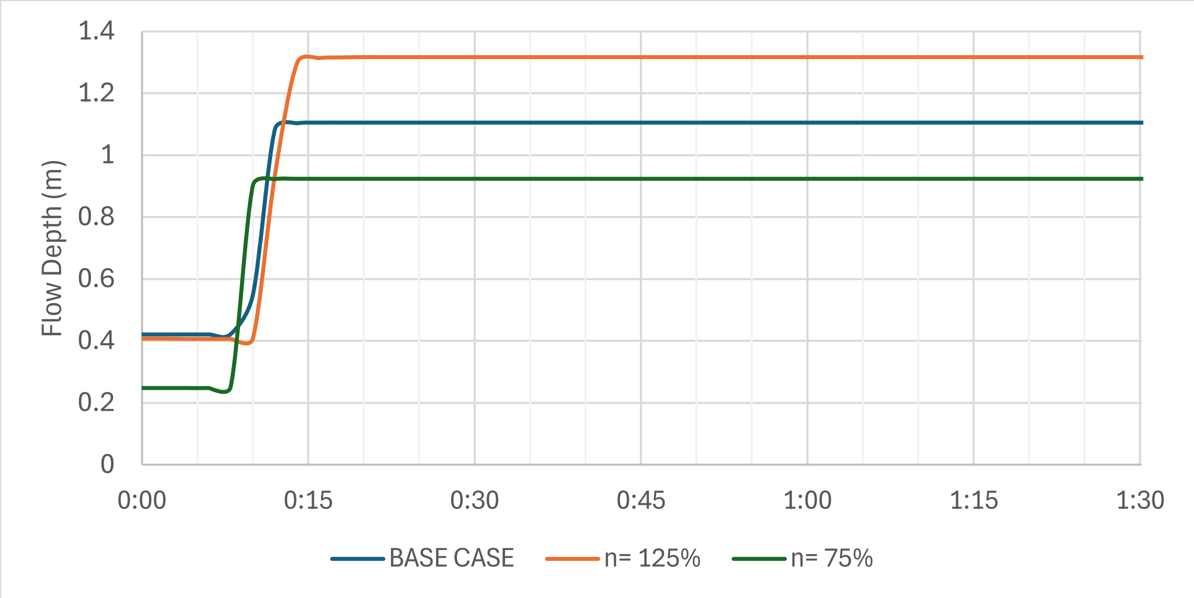

Figure B-1: Flow depth changes with various roughness (Manning n) assumptions following station shutdown (no bypass, $Q_{WAITAHA}$ = 26.5 m^3/s) at Morgan Gorge hot spring (ch. 810)

Table B-1: Flow depth changes with various roughness (Manning n) assumptions following station shutdown (no bypass, $Q_{WAITAHA}$ = 26.5 m^3/s) at Morgan Gorge hot spring (ch. 810)

Roughness n	ΔD	Time to D_{MAX}
BASE CASE	0.68 m	14 min
125%	0.91 m	16 min
75%	0.68 m	12 min

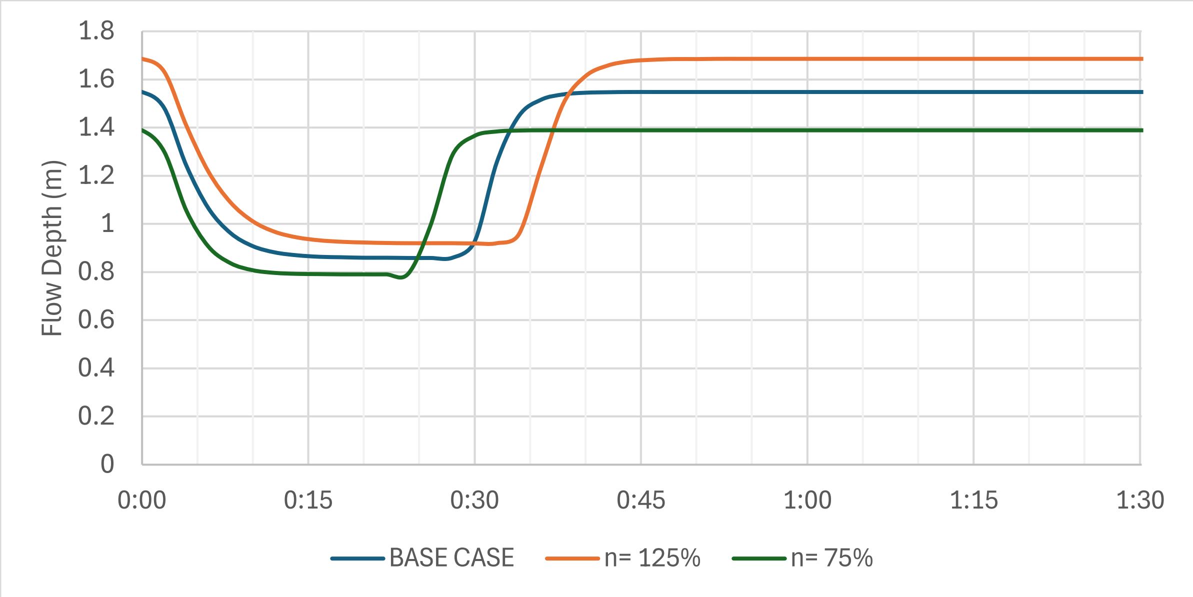

Figure B-2: Flow depth changes with various roughness (Manning n) assumptions following station shutdown (no bypass, $Q_{WAITAHA}$ = 26.5 m^3/s) at ch. 2500

Table B-2: Flow depth changes with various roughness (Manning n) assumptions following station shutdown (no bypass, $Q_{WAITAHA}$ = 26.5 m^3/s) at ch. 2500

Roughness n	***ΔD***	***Time to 95% ΔD***	***Time to recovery (5% ΔD)***
BASE CASE	*0.69 m*	*12 min*	*36 min*
125%	*0.77 m*	*14 min*	*42 min*
75%	*0.60 m*	*10 min*	*30 min*

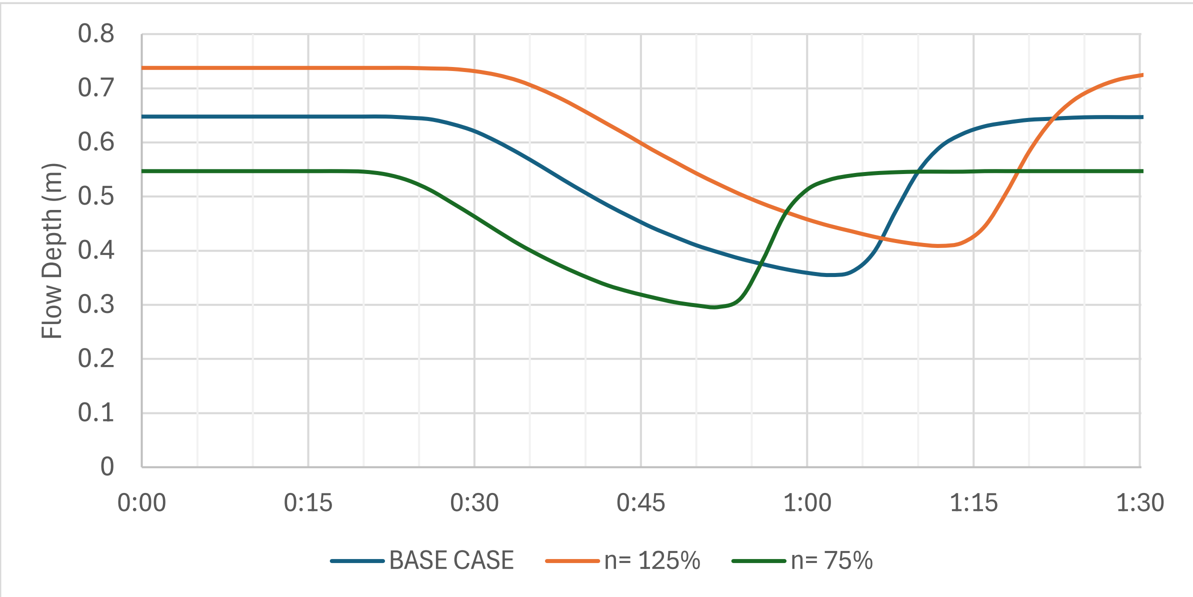

Figure B-3: Flow depth changes with various roughness (Manning n) assumptions following station shutdown (no bypass, $Q_{WAITAHA}$ = 26.5 m^3/s) at ch. 5000

Table B-3: Flow depth changes with various roughness (Manning n) assumptions following station shutdown (no bypass, $Q_{WAITAHA}$ = 26.5 m^3/s) at ch. 5000

Roughness n	ΔD	Time to 95% ΔD	Time to recovery (5% ΔD)
BASE CASE	0.29 m	58 min	78 min
125%	0.33 m	68 min	90 min
75%	0.25 m	48 min	64 min

Appendix C –Model Results - Flow Changes For Controlled Shutdown

For controlled station flow rampdown, the minimum flow in the Waitaha River is presented at key locations in Table C-1 and through the modelled reach in Figures C-1 to C-3 below.

Table C-1: Minimum flow in Waitaha River following full load power station flow rampdown

River Flow $Q_{WAITAHA}$	Power Station	Downstream station	Start of braiding	Model extent
		ch. 2500	ch. 5000	ch. 10000
16.5 m³/s	*Initial Generation Flow*	17.5 m^3/s	21.3 m^3/s	21.3 m^3/s
	30 min ramp down	4.8	10.0	13.0
	45 min ramp down	6.4	11.4	13.6
	60 min ramp down	9.0	13.4	14.6
26.5 m³/s	*Initial Generation Flow*	28.2	34.1	34.1
	30 min ramp down	5.7	14.7	19.6
	45 min ramp down	10.3	18.1	21.1
	60 min ramp down	14.3	21.4	23.1
36.5 m³/s	*Initial Generation Flow*	38.7	47.0	47.0
	30 min ramp down	19.9	30.3	33.9
	45 min ramp down	25.3	34.2	35.8
	60 min ramp down	28.6	37.2	38.0

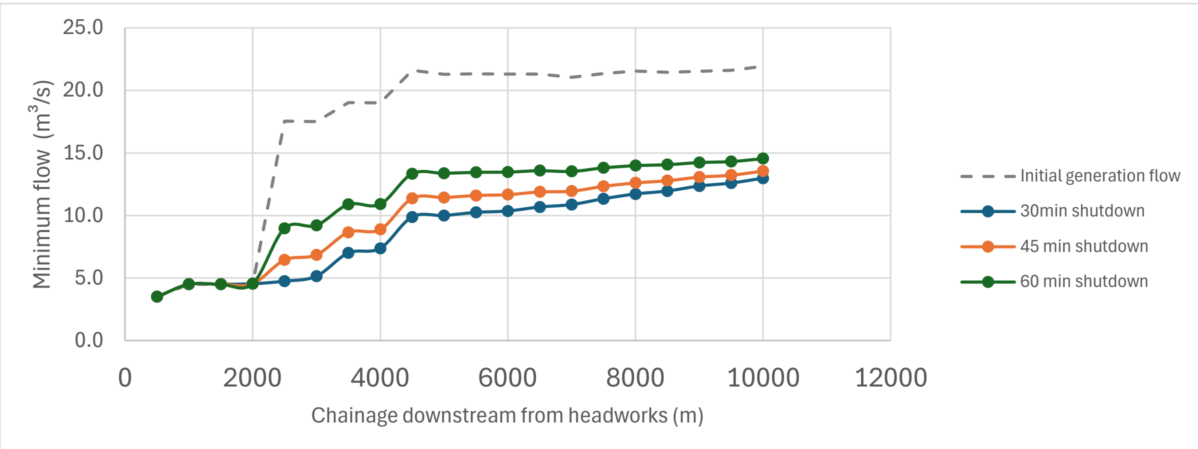

Figure C-1: Minimum flow in Waitaha River following full station shutdown (16.5 m^3/s at headworks)

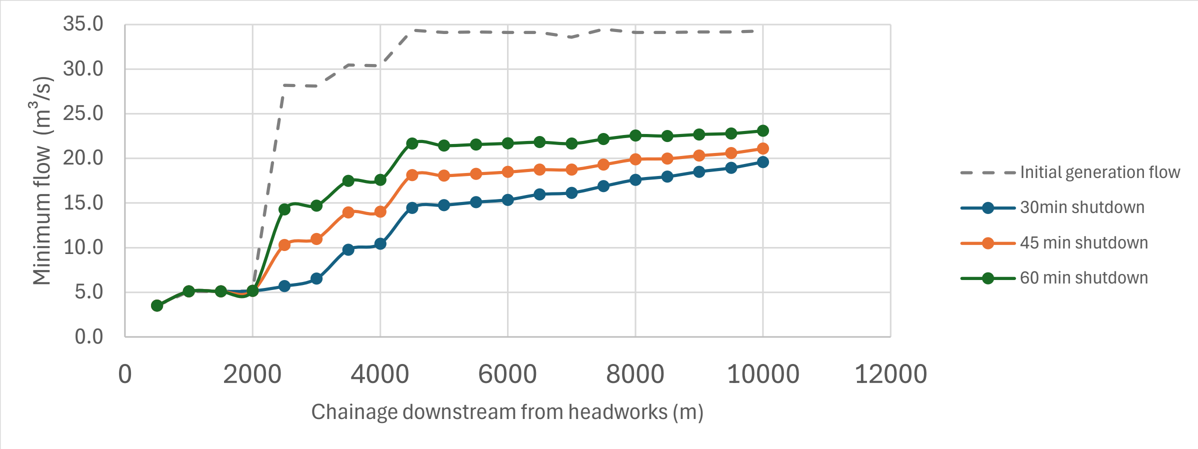

Figure C-2: Minimum flow in Waitaha River following full station shutdown (26.5 m^3/s at headworks)

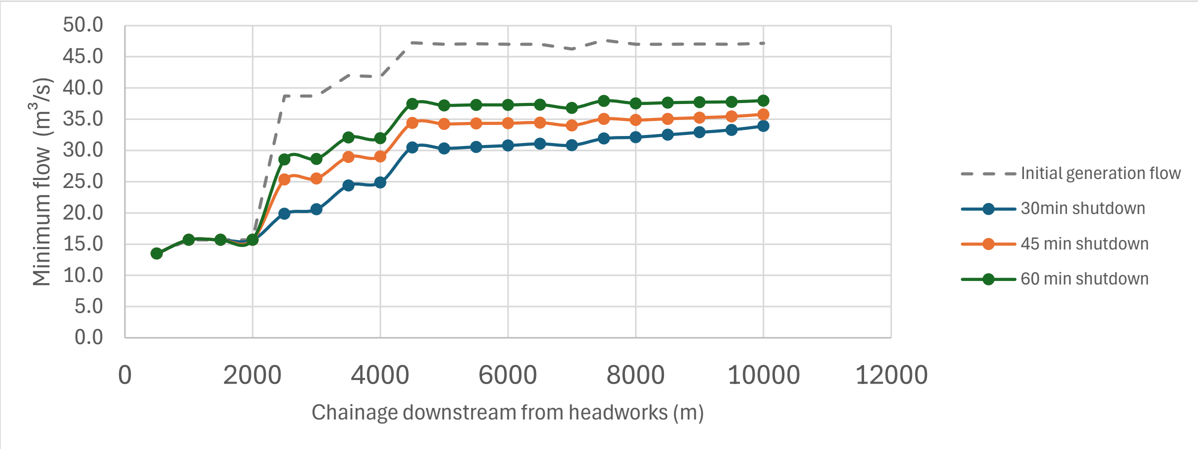

Figure C-3: Minimum flow in Waitaha River following full station shutdown (36.5 m^3/s at headworks)

For the modelled case of 16.5 m^3/s at the headworks and the station flow of 13 m^3/s being gradually ramped down, river flow for 2-4 km downstream of the station temporarily drops below 50% for ramping times of 30 minutes (0.43 m^3/s per minute) and 45 minutes (0.28 m^3/s per minute) as shown in Figure C-4, and does not drop below 50% for the 60 minute rampdown.

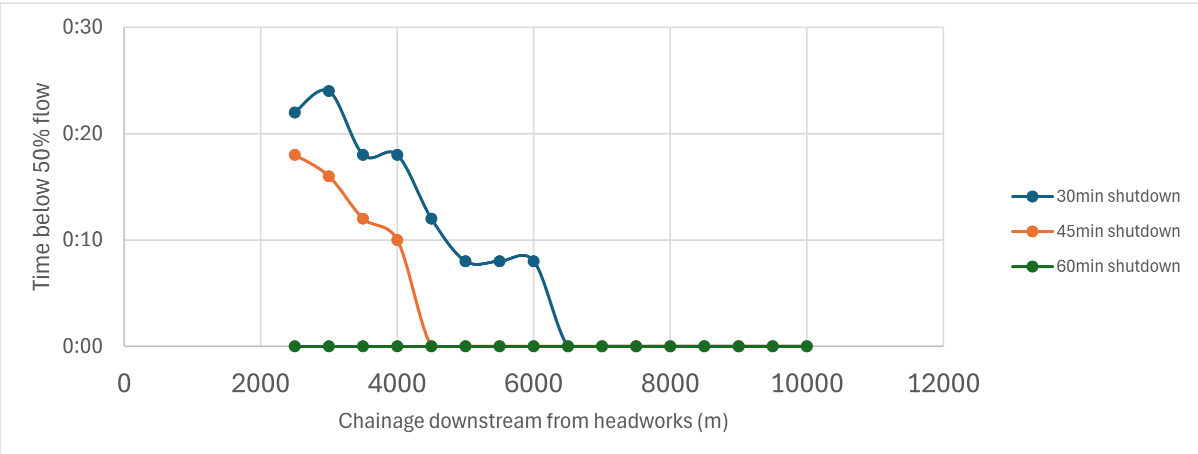

Figure C-4: Time that river flow is below 50% of steady-state for 16.5 m^3/s at headworks, following controlled shutdown of station flow (13 m^3/s) over 30 minutes, 45 minutes and 60 minutes.

Rates of change of flow for the slower controlled station flow reduction cases are shown in Table C-2 (maximum rate of change of flow reduction) and Table C-3 (maximum rate of change of flow increase).

*Table C-2: Maximum rate of change of flow **reduction** in Waitaha River following controlled shutdown (m^3/s per minute)*

River Flow $Q_{WAITAHA}$	Power Station	Downstream headworks	Downstream station	Start of braiding	Model extent
		ch. 500	ch. 2500	ch. 5000	ch. 10000
16.5 m^3/s	30 min ramp down	0.0 m^3/s/min	0.4 m^3/s/min	0.3 m^3/s/min	0.2 m^3/s/min
	45 min ramp down	-	0.3	0.2	0.2
	60 min ramp down	-	0.2	0.2	0.1
26.5 m^3/s	30 min ramp down	-	0.7	0.5	0.4
	45 min ramp down	-	0.5	0.4	0.3
	60 min ramp down	-	0.4	0.3	0.3
36.5 m^3/s	30 min ramp down	-	0.8	0.6	0.4
	45 min ramp down	-	0.5	0.4	0.3
	60 min ramp down	-	0.4	0.3	0.3

*Table C-3: Maximum rate of change of flow **increase** in Waitaha River following controlled shutdown (m^3/s per minute)*

River Flow $Q_{WAITAHA}$	Power Station	Downstream headworks	Downstream station	Start of braiding	Model extent
		ch. 500	ch. 2500	ch. 5000	ch. 10000
16.5 m^3/s	30 min ramp down	0.6 m^3/s/min	0.9 m^3/s/min	1.0 m^3/s/min	0.4 m^3/s/min
	45 min ramp down	0.4	0.5	0.5	0.3
	60 min ramp down	0.3	0.3	0.3	0.2
26.5 m^3/s	30 min ramp down	1.2	2.0	2.0	0.7
	45 min ramp down	0.7	0.7	0.9	0.5
	60 min ramp down	0.5	0.4	0.5	0.4
36.5 m^3/s	30 min ramp down	0.8	1.1	1.1	0.6
	45 min ramp down	0.5	0.6	0.6	0.4
	60 min ramp down	0.4	0.4	0.4	0.3

Appendix D –Flow Depth Changes For Controlled Shutdown and Startup Cases

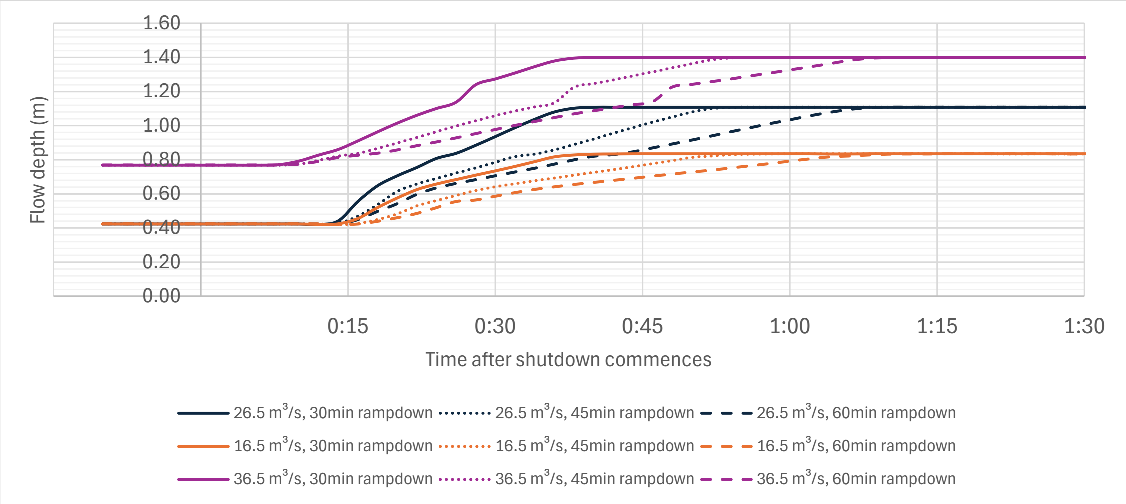

Figure D-1: Flow depth changes following station shutdown at Morgan Gorge hot spring (ch. 810)

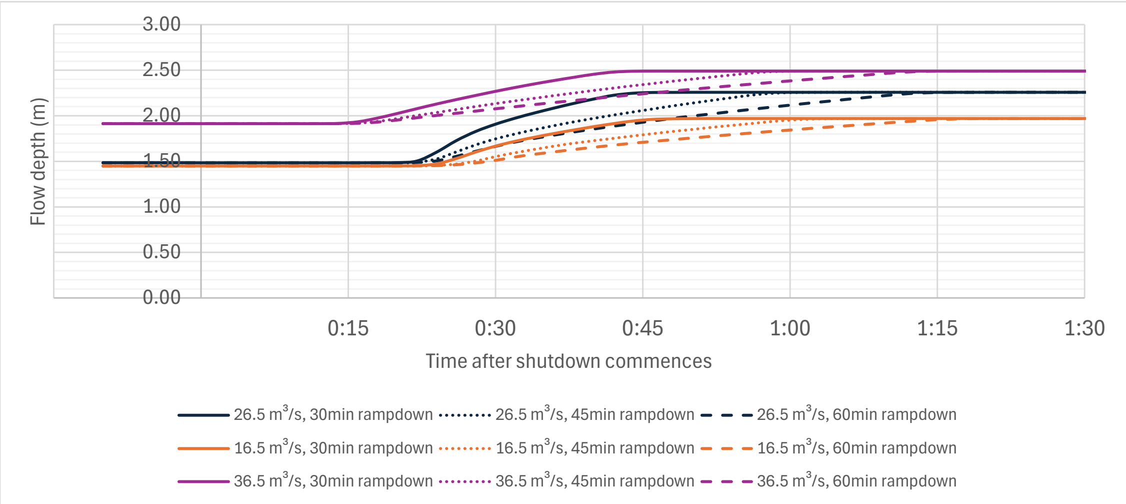

Figure D-2: Flow depth changes following station shutdown downstream of Morgan Gorge (ch. 1500)

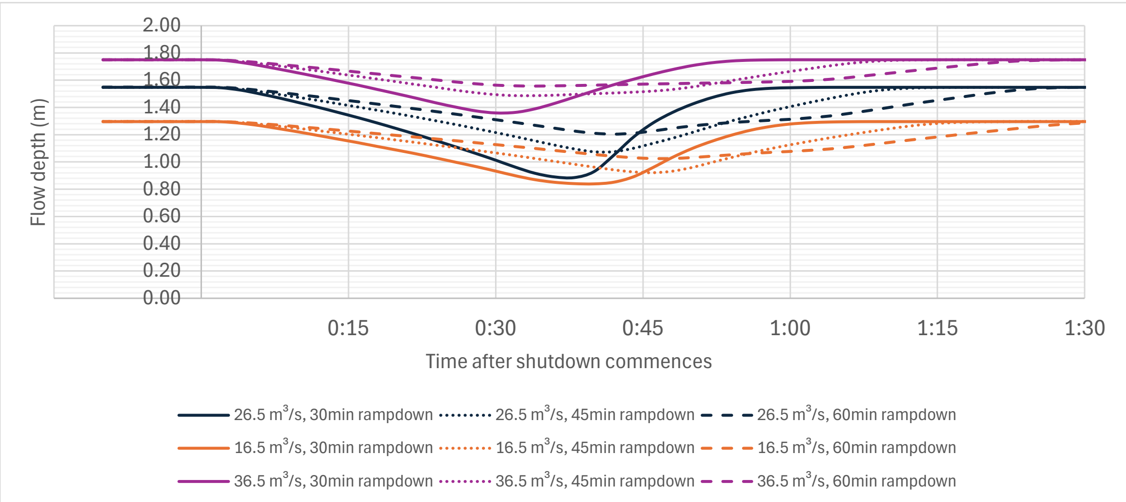

Figure D-3: Flow depth changes following station shutdown downstream of power station (ch. 2500)

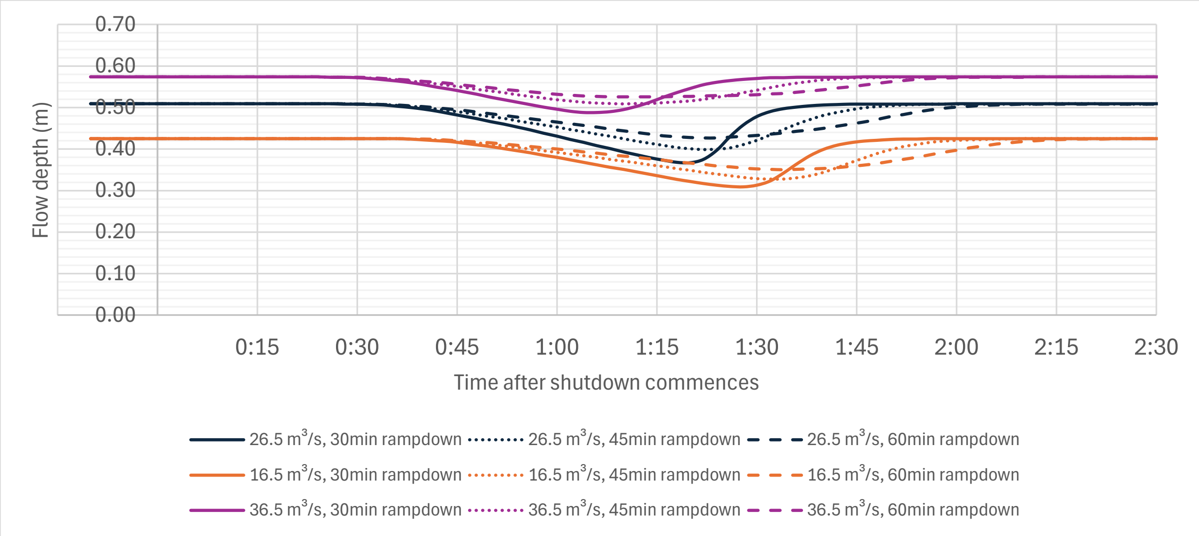

Figure D-4: Flow depth changes following station shutdown upstream of braided reach (ch. 5400)

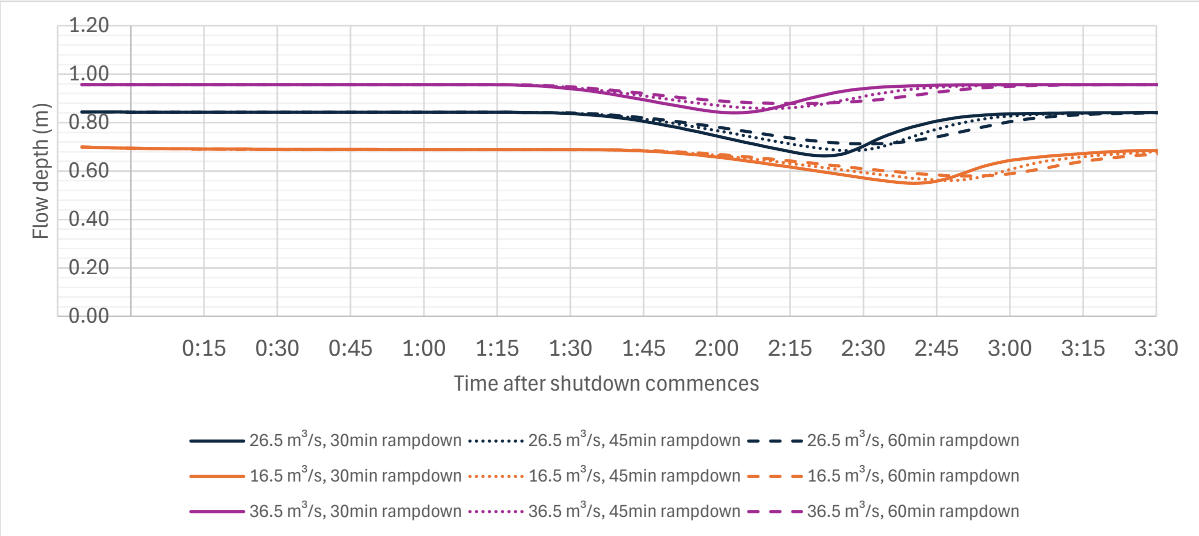

Figure D-5: Flow depth changes following station shutdown near downstream model boundary (ch. 10180)

Table D-1: Steady-state depth mid-channel (before station shutdown) and maximum/minimum depth following station shutdown for $Q_{WAITAHA}$***=26.5 m³/s,*** *30min rampdown, 45min rampdown, 60min rampdown*

Chainage	D_{STEADY}	D_{MAX} (30min rampdown)	D_{MAX} (45min rampdown)	D_{MAX} (60min rampdown)
810	0.42 m	1.11 m	1.11 m	1.11 m
1500	1.48	2.26	2.26	2.26
		D_{MIN} (30min rampdown)	D_{MIN} (45min rampdown)	D_{MIN} (60min rampdown)
2500	1.55	0.89	1.08	1.20
5400	0.51	0.37	0.40	0.43
10180	0.84	0.66	0.69	0.71

Table D-2: Steady-state depth mid-channel (before station shutdown) and maximum/minimum depth following station shutdown for $Q_{WAITAHA}$***=16.5 m³/s,*** *30min rampdown, 45min rampdown, 60min rampdown*

Chainage	D_{STEADY}	D_{MAX} (30min rampdown)	D_{MAX} (45min rampdown)	D_{MAX} (60min rampdown)
810	0.42 m	0.84 m	0.84 m	0.84 m
1500	1.45	1.97	1.97	1.97
		D_{MIN} (30min rampdown)	D_{MIN} (45min rampdown)	D_{MIN} (60min rampdown)
2500	1.30	0.84	0.92	1.03
5400	0.43	0.31	0.33	0.35
10180	0.70	0.55	0.56	0.58

Table D-3: Steady-state depth mid-channel (before station shutdown) and maximum/minimum depth following station shutdown for $Q_{WAITAHA}$***=36.5 m³/s,*** *30min rampdown, 45min rampdown, 60min rampdown*

Chainage	D_{STEADY}	D_{MAX} (30min rampdown)	D_{MAX} (45min rampdown)	D_{MAX} (60min rampdown)
810	0.77 m	1.40 m	1.40 m	1.40 m
1500	1.91	2.49	2.49	2.49
		D_{MIN} (30min rampdown)	D_{MIN} (45min rampdown)	D_{MIN} (60min rampdown)
2500	1.75	1.36	1.49	1.56
5400	0.57	0.49	0.51	0.53
10180	0.96	0.84	0.86	0.88

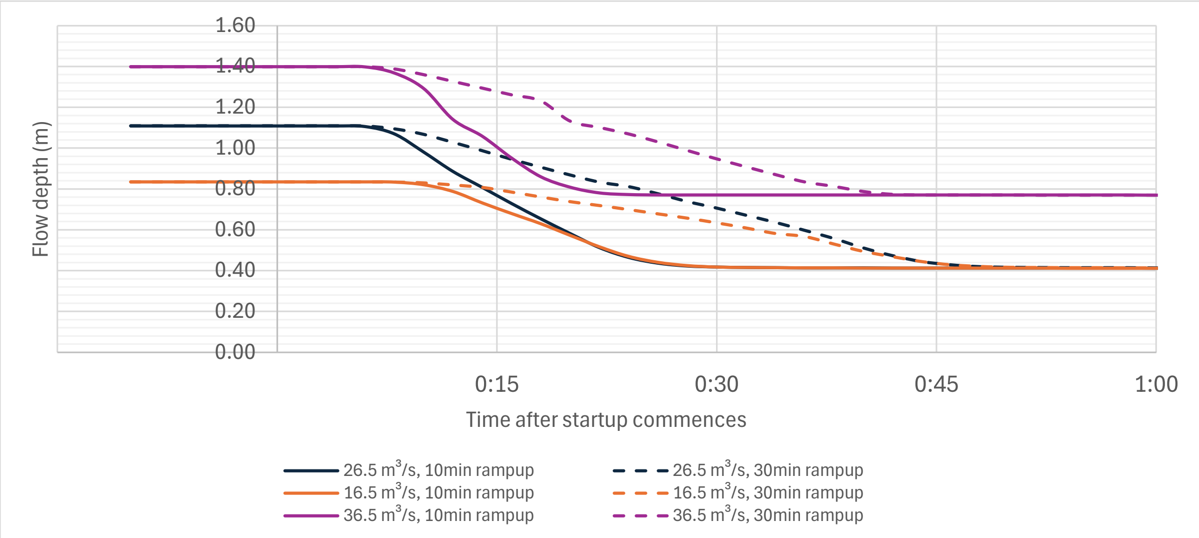

Figure D-6: Flow depth changes following station startup at Morgan Gorge hot spring (ch. 810)

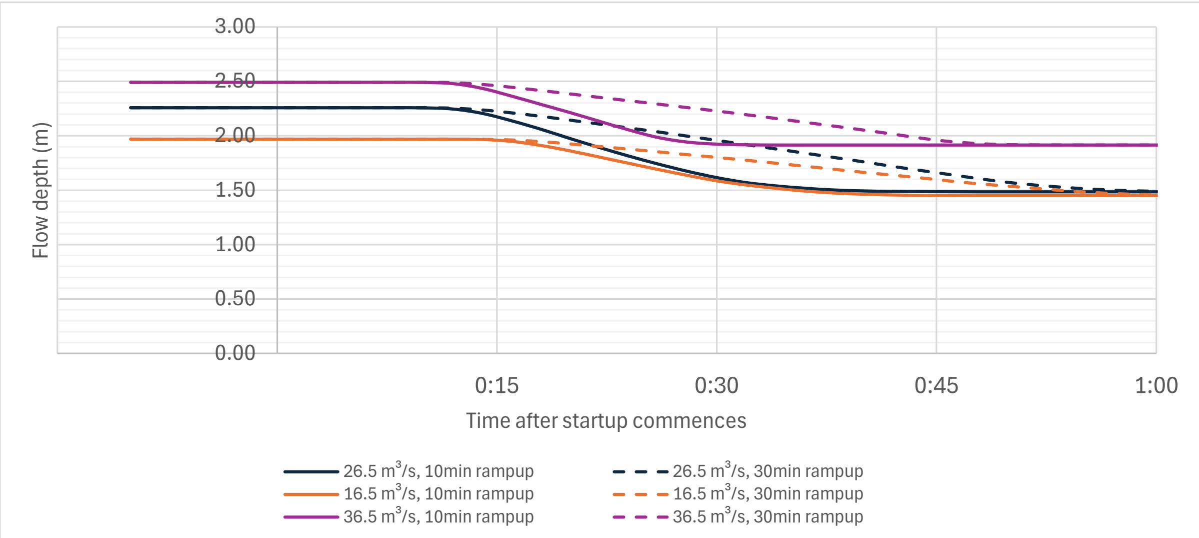

Figure D-7: Flow depth changes following station startup downstream of Morgan Gorge (ch. 1500)

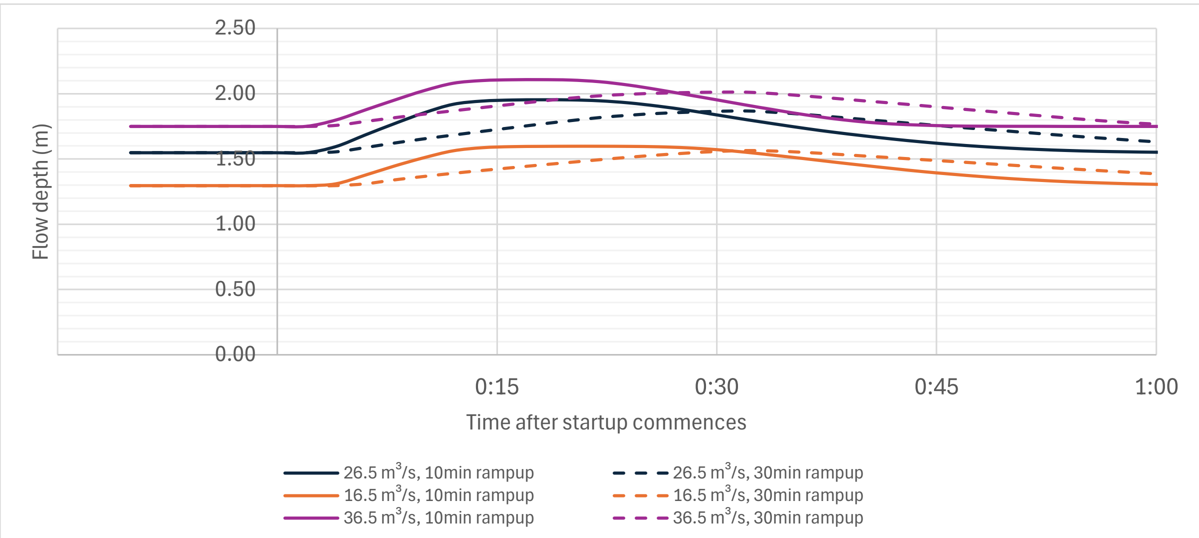

Figure D-8: Flow depth changes following station startup downstream of power station (ch. 2500)

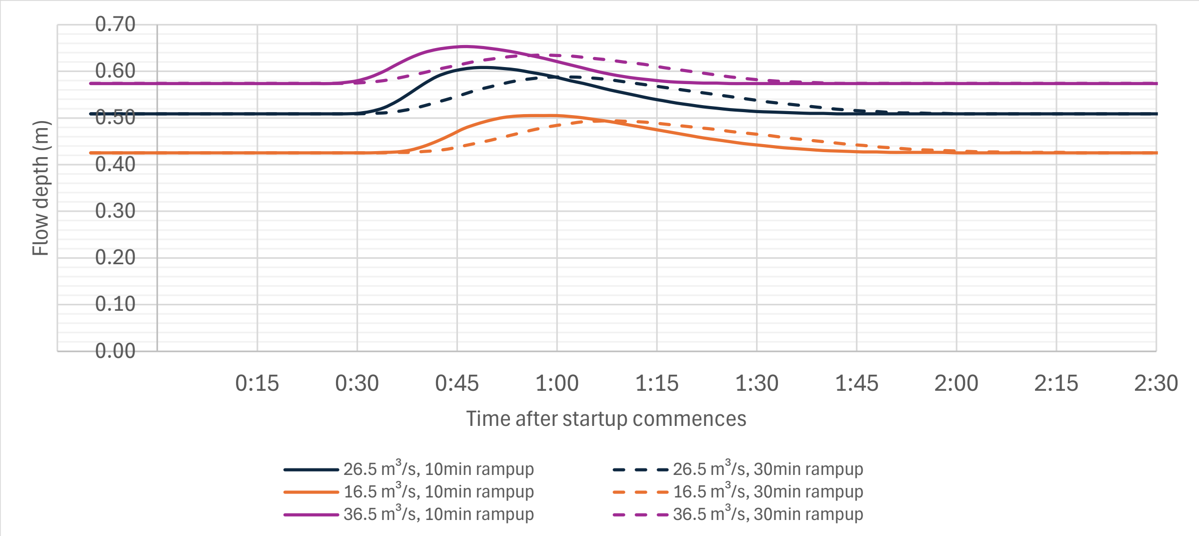

Figure D-9: Flow depth changes following station startup upstream of braided reach (ch. 5400)

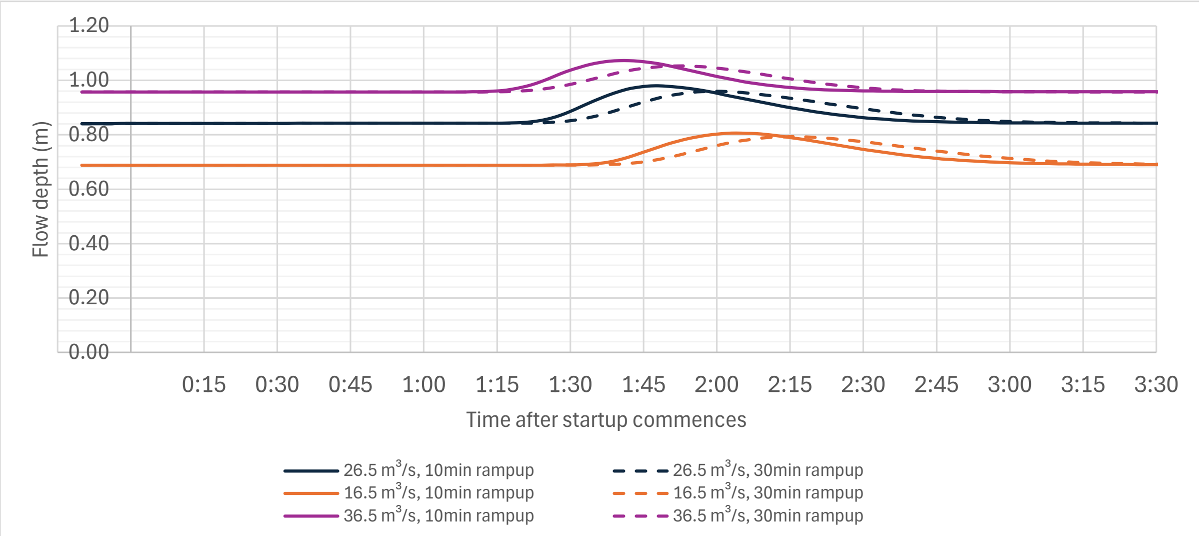

Figure D-10: Flow depth changes following station startup near downstream model boundary (ch. 10180)

Table D-4: Steady-state depth mid-channel (before station startup) and maximum/minimum depth following station startup for $\boldsymbol{Q_{WAITAHA}=26.5\ m^3/s}$, *10min rampup, 30min rampup*

Chainage	D_{STEADY}	D_{MIN} (10min rampup)	D_{MIN} (30min rampup
810	1.11 m	0.40 m	0.40 m
1500	2.26	1.48	1.48
		D_{MAX} (10min rampup)	D_{MAX} (30min rampup)
2500	1.55	1.95	1.87
5400	0.51	0.61	0.59
10180	0.84	0.98	0.96

Table D-5: Steady-state depth mid-channel (before station startup) and maximum/minimum depth following station startup for $\boldsymbol{Q_{WAITAHA}=16.5\ m^3/s}$, *10min rampup, 30min rampup*

Chainage	D_{STEADY}	D_{MIN} (10min rampup)	D_{MIN} (30min rampup
810	0.84 m	0.40 m	0.40 m
1500	1.97	1.45	0.45
		D_{MAX} (10min rampup)	D_{MAX} (30min rampup)
2500	1.30	1.60	1.57
5400	0.43	0.51	0.49
10180	0.69	0.81	0.79

Table D-6: Steady-state depth mid-channel (before station startup) and maximum/minimum depth following station startup for $\boldsymbol{Q_{WAITAHA}=36.5\ m^3/s}$, *10min rampup, 30min rampup*

Chainage	D_{STEADY}	D_{MIN} (10min rampup)	D_{MIN} (30min rampup
810	1.40 m	0.77 m	0.77 m
1500	2.49	1.91	1.91
		D_{MAX} (10min rampup)	D_{MAX} (30min rampup)
2500	1.75	2.11	2.01
5400	0.57	0.65	0.64
10180	0.96	1.07	1.05